

January 2008

Domain Effects in the Finite / Infinite Time Stability Properties of a Viscous Shear Flow Discontinuity

Kranthi Kumar Kolli

University of Massachusetts Amherst, kranthi.kolli@gmail.com

Follow this and additional works at: <http://scholarworks.umass.edu/theses>

Kolli, Kranthi Kumar, "Domain Effects in the Finite / Infinite Time Stability Properties of a Viscous Shear Flow Discontinuity" (2008). *Masters Theses 1911 - February 2014*. 204.

<http://scholarworks.umass.edu/theses/204>

This thesis is brought to you for free and open access by the Dissertations and Theses at ScholarWorks@UMass Amherst. It has been accepted for inclusion in Masters Theses 1911 - February 2014 by an authorized administrator of ScholarWorks@UMass Amherst. For more information, please contact scholarworks@library.umass.edu.

**DOMAIN EFFECTS IN THE FINITE/INFINITE TIME
STABILITY PROPERTIES OF A VISCOUS SHEAR
FLOW DISCONTINUITY**

A Thesis Presented

by

KRANTHI KUMAR KOLLI

Submitted to the Graduate School of the
University of Massachusetts Amherst in partial fulfillment
of the requirements for the degree of

MASTER OF SCIENCE IN MECHANICAL ENGINEERING

September 2008

Mechanical and Industrial Engineering

© Copyright by Kranthi Kumar Kolli 2008

All Rights Reserved

**DOMAIN EFFECTS IN THE FINITE/INFINITE TIME
STABILITY PROPERTIES OF A VISCOUS SHEAR
FLOW DISCONTINUITY**

A Thesis Presented

by

KRANTHI KUMAR KOLLI

Approved as to style and content by:

Kumar M. Bobba, Chair

David P. Schmidt, Member

Yossi Chait, Member

Mario Rotea, Department Chair
Mechanical and Industrial Engineering

ACKNOWLEDGMENTS

I would like to express my sincere gratitude to Professor Kumar M Bobba, for his constant guidance and support during the course of my M.S. study at the University of Massachusetts, Amherst. His patience, knowledge and constant encouragement helped me learn, improve and enjoy my work at the Complex Flow and Automatic Control (CoFAC) Laboratory. It is his deep understanding of the nature of the technical challenges that has enabled me to focus on what was essential and critical towards the successful completion of my M.S. degree study. With his help, I have not only improved my research capabilities, but also my way of thinking and communicating. I believe the training I have received under his direction will greatly benefit my future career.

I would also like to thank Professor David P. Schmidt and Professor Yossi Chait for serving on my thesis committee and providing valuable feedback on my research work.

I had lot of fun times with my friends at UMASS, Nishanth, Russell Kondaveti, Harsha, ARK, Avi, Kapil, Kaustubh, Rajiv, Steve, Sripati, Abhijit and Rajaram. It was always nice talking to them, their practical advice has been very useful on many occasions. Thanks to them all.

And, a special thank you to my parents for their support and encouragement without which I would not have been where I am today.

Finally I would like to gratefully acknowledge funding provided to this research by the National Science Foundation under grant CBET 0631280.

ABSTRACT

DOMAIN EFFECTS IN THE FINITE/INFINITE TIME STABILITY PROPERTIES OF A VISCOUS SHEAR FLOW DISCONTINUITY

SEPTEMBER 2008

KRANTHI KUMAR KOLLI

B.E.M.E., OSMANIA UNIVERSITY, HYDERABAD, INDIA

M.S.M.E., UNIVERSITY OF MASSACHUSETTS AMHERST

Directed by: Professor Kumar M. Bobba

Whether it is designing and controlling super-efficient high speed transport systems or understanding environmental fluid flows, a key question that arises is: what state does the fluid flow take and why? An answer to this question lies in understanding the hydrodynamic stability properties of the flow as a function of parameters. While much work has been done in this area in the past, there are many open questions that need to be addressed. Here we study the effect of spatial domain size, number of modes, non-hermitianness and non-normality on the finite time and infinite time stability properties of a standing, viscous, shock flow problem.

It has been shown that the above problems are not only non-normal but also non-hermitian, when the base flow has shear. The eigenvalue problems corresponding to infinite spatial domain, finite spatial domain, forward and L_2 adjoint problems are solved exactly by converting the linear partial differential equations into nonlinear

Riccati equations. In the finite domain case, the full time dependent solutions are obtained analytically using the bi-orthogonal basis functions.

In the infinite spatial domain case, the point spectrum of the forward operator is shown to be unbounded and that of the adjoint operator to be empty. In the unbounded case, the spectrum fills the entire area on one side of a parabola in the complex plane and is connected. As the fluid viscosity decreases, the width of the parabola increases and in the limit of zero viscosity covers almost the entire left half plane. On the other hand, as the fluid viscosity increases, the width of the parabola decreases and in the limit of infinite viscosity becomes the negative real axis, which is the spectrum of the heat equation. The spectrum of the adjoint problem is empty for all values of the viscosity and prescribed velocity.

In the finite spatial domain case, the point spectrum lies in the open left half plane for all the Reynolds numbers and hence asymptotically stable. The results shown that perturbations grow substantially large for finite time before they decay at large times. It is also found that retaining right number of modes is crucial for observing transient growth phenomena. Finally, the linear results are compared with the nonlinear finite amplitude simulation results.

The relevance of current results to other fluid flows is also presented.

TABLE OF CONTENTS

	Page
ACKNOWLEDGMENTS	iv
ABSTRACT	v
LIST OF TABLES	ix
LIST OF FIGURES	x
CHAPTER	
1. INTRODUCTION	1
1.1 Linear Stability Theory	1
1.2 Weakly Nonlinear Theory	2
1.3 Finite Amplitude Disturbances	3
1.4 Transient Algebraic Growth	3
1.4.1 Non-normal Effects	4
1.5 Present Thesis	7
2. DISSIPATING SHOCK WAVE EQUATION	8
2.1 Motivation	8
2.2 Time Independent Nonlinear Base State	9
3. SPECTRUM OF THE DISCONTINUITY IN THE INFINITE DOMAIN	11
3.1 Base Flow Structure	12
3.2 Forward Evolution Operator	12
3.3 Definition of the Inner Product Space	13
3.4 Adjoint Evolution Operator: Non Hermitianness and Non-normality	13
3.5 Non-dimensionalization	14

3.6	Point Spectrum of the Adjoint Operator	15
3.7	Point Spectrum of the Forward Operator	20
3.8	Spectrum Variation with Viscosity and Baseflow	25
3.9	Discussion	27
4.	STABILITY OF THE DISCONTINUITY IN THE FINITE DOMAIN	28
4.1	Linearized Forward Disturbance Equation	28
4.2	Adjoint Disturbance Equation	30
4.3	Non-Normality and Non-Hermitian Properties	31
4.4	Non-Dimensionalization	31
4.5	Eigen Spectrum of the Adjoint Operator	32
4.5.1	Eigen Functions of the Adjoint Operator	34
4.6	Eigen Spectrum for the Forward Operator	41
4.6.1	Eigen Functions of the Forward Operator B	42
4.7	Discussion	48
5.	EXACT SOLUTIONS USING BI-ORTHOGONAL BASIS FUNCTIONS	49
5.1	Orthogonality and Bi-orthogonality	49
5.2	Solution of the Linear Equations	50
5.3	Numerical Simulations: Effect of the Number of Modes and the Initial Conditions on the Transient Growth	51
5.4	Discussion	54
6.	NON-LINEAR FINITE AMPLITUDE EFFECTS	55
6.1	Projection of the Equations on to a Finite Dimensional Space	55
6.2	Three Mode Subspace	56
6.3	Comparison of Linear and Nonlinear Energy Growth	58
6.4	Velocity Evolution With Time and Space	62
7.	CONCLUSION AND SUMMARY OF MAIN RESULTS	66
	BIBLIOGRAPHY	68

LIST OF TABLES

Table	Page
4.1 Eigen Values of B^* in the finite domain case	39
4.2 Eigen Values of B in the finite domain case	45
6.1 Numerically computed values of γ_{ijk}	57

LIST OF FIGURES

Figure	Page
2.1 Plot of steady state solution for different viscosity values	10
3.1 First eigenfunction $\psi_1^{(b)}(y)$ of B corresponding to $\lambda = -1 + i$. The real part is shown in solid line and the imaginary part in dashed line. Horizontal axis is the spatial co-ordinate y	22
3.2 Second eigenfunction $\psi_2^{(b)}(y)$ of B corresponding to $\lambda = -1 + i$. The real part is shown in solid line and the imaginary part in dashed line. Horizontal axis is the spatial co-ordinate y	23
3.3 The eigenvalue spectrum of the infinite dimensional operator B in the complex plane.	24
3.4 Effect of Fluid viscosity on the spectrum S_Θ in the complex plane. The area on the left of the dashed line is for $\frac{a^2}{\nu} = 5$, the area on the left of solid line is for $\frac{a^2}{\nu} = 1$, the area on the left of dotted line is for $\frac{a^2}{\nu} = 0.1$. Symmetry of each curve with $Re[\theta]$ is shown in different colors.	25
4.1 Plot of steady state solution for different viscosity values	29
4.2 Plot showing eigenvalue μ_1 calculation for Case (c), for k_1 Real.	37
4.3 Plot showing eigenvalue's μ_2, \dots, μ_6 calculated for Case (c) with k_2, \dots, k_6 being purely complex.	38
4.4 Plot of eigenvalues of the adjoint operator B^*	38
4.5 The eigenfunction of the finite dimensional operator B^* corresponding to eigenvalue μ_1	39
4.6 The eigenfunction of the finite dimensional operator B^* corresponding to eigenvalue μ_2	40
4.7 The eigenfunction of the finite dimensional operator B^* corresponding to eigenvalue μ_3	40

4.8	Plot of the eigenvalues of the forward operator B	46
4.9	The eigenfunction of the finite dimensional operator B corresponding to the eigenvalue λ_1	46
4.10	The eigenfunction of the finite dimensional operator B corresponding to the eigenvalue λ_2	47
4.11	The eigenfunction of the finite dimensional operator B corresponding to the eigen value λ_3	47
5.1	Plot of energy variation with time. Solid line represents $N=2$ modes and dashed line represents $N=3$ modes. For a specific notation we observe that in both the above cases energy decreases monotonically	53
5.2	Plot of energy variation with time. Solid line represents $N=2$ modes and dashed line represents $N=3$ modes. For a specific notation we observe that, while the energy of 2 modes decreases monotonically, and that of three mode system grows transiently	54
6.1	Energy variation with time for linear and nonlinear governing equations. The initial condition for the simulations are $p_{1_0} = 2.6, p_{2_0} = 0, p_{3_0} = -1.3$	58
6.2	Energy variation with time for linear and nonlinear governing equations. The initial condition for the simulations are $p_{1_0} = 1.0, p_{2_0} = 0, p_{3_0} = -0.5$	59
6.3	Variation of $p_1(t)$ coefficient in the linear and nonlinear simulations of Figure (6.1)	59
6.4	Variation of $p_2(t)$ coefficient in the linear and nonlinear simulations of Figure (6.1). Notice that the IC for $p_2[t]$ is zero and hence remains at zero in the linear case as the system is diagonal and decoupled.	60
6.5	Variation of $p_3(t)$ coefficient in the linear and nonlinear simulations of Figure (6.1)	60
6.6	Variation of $p_1(t)$ coefficient in the linear and nonlinear simulations of Figure (6.2)	61

6.7	Variation of $p_2(t)$ coefficient in the linear and nonlinear simulations of Figure (6.2). Notice that the IC for $p_2[t]$ is zero and hence remains at zero in the linear case as the system is diagonal and decoupled.	61
6.8	Variation of $p_3(t)$ coefficient in the linear and nonlinear simulations of Figure (6.2).....	62
6.9	Plot showing the variation of velocity with respect to space for the linear and non-linear cases of Figure (6.1) at time $t=0$. The base flow is also plotted for reference in this and other figures next.	63
6.10	Plot showing the variation of velocity with respect to space for the linear and non-linear cases of Figure (6.1) at time $t=1$	63
6.11	Plot showing the variation of velocity with respect to space for the linear and non-linear cases of Figure (6.1) at time $t=20$	64
6.12	Plot showing the variation of velocity with respect to space for the linear and non-linear cases of Figure (6.1) at time $t=40$	64

CHAPTER 1

INTRODUCTION

Flow stability theory plays a central role in our physical, theoretical and computational understanding of fluid flow instabilities, transition to turbulence and even fully developed turbulence. These in turn are related to many of the practical questions designers are interested like, resistance, rate of mixing between different fluids, heat transfer and others. Hydrodynamic stability theory [1] has received a great deal of attention over the past decades and is still a field of active and ongoing research because of many yet to be answered questions.

1.1 Linear Stability Theory

The basic strategy in studies of hydrodynamic stability [1] is to understand the effects of disturbances on a steady mean flow. In linear theory the disturbances are assumed to be small and the nonlinear terms of the equations governing the disturbances are neglected. The traditional way of analyzing the linearized problem has been a normal mode approach resulting in an eigenvalue problem. For pipe flow the assumption is a streamwise (x), azimuthal (ϕ) and time dependence of form $\exp i(\alpha(x - ct) + n\phi)$, where α and n are the streamwise and azimuthal wavenumbers and c is the complex wave speed. For planar flows the corresponding form is $\exp i(\alpha(x - ct) + \beta z)$ where z is the spanwise coordinate and β is the corresponding wavenumber. If α and β is real c will be complex and is determined from a (temporal) eigenvalue problem. The imaginary part of c determines whether the perturbations are damped ($c_i < 0$),

neutrally stable ($c_i = 0$) or growing ($c_i > 0$). If the frequency is kept real as it would be in a vibrating ribbon experiment, α becomes the complex (spatial) eigenvalue.

Linear stability is defined in an asymptotic manner as $t \rightarrow \infty$. If for a given value of the flow parameters any, sufficiently small perturbation dies out, the system is said to be linearly stable for this particular choice of parameters. In the case of exponentially growing perturbations, the system is linearly unstable and nonlinear effects will become significant once initially small perturbations reach sufficient amplitudes.

When the theoretical predictions of stability are compared with experimental observations of transition to turbulence, in most cases some discrepancies are observed. In pipe flow experiments, transition has been found to occur for Reynolds numbers down to about *2000* (Wyganski et. al. [2]), but flow may remain laminar even at considerable larger values. In plane Poiseuille flow [3], the lowest Reynolds number for transition observed is about *1000* and in plane Couette flow [4] transition occurs at $Re=360$. The conclusion drawn from the above is that the linear eigenvalue problem is in general not capable of predicting all the aspects of transition. The discrepancy between the predictions of linear theory and experimental observations has then naturally focused the interest on nonlinear effects.

1.2 Weakly Nonlinear Theory

If the disturbances are considered to be finite in amplitude, nonlinearities are introduced in governing equations. In an examination whether finite-amplitude equilibrium waves exist in viscous shear flows, Noether noticed that the mean flow profile becomes distorted owing to action of Reynolds stresses if a steady wave is present. This implication was further developed for Plane Poiseuille flow by Meksyn and Stuart [5], who derived approximate solutions to Noether's equations.

By including nonlinear terms and expanding the governing equations in powers of disturbance amplitude, Stuart and Watson [6] derived evolution equations for the

amplitude. The equations are of Landau [7] type and the effect of nonlinearity is then essentially determined by sign of coefficients (Landau coefficients) of nonlinear terms. For plane Poiseuille flow [8, 9] calculated the first Landau coefficient and found that plane Poiseuille flow is subcritically unstable, i.e. becomes unstable at a lower Reynolds number than found in linear theory.

1.3 Finite Amplitude Disturbances

In global theories, arbitrary large disturbances are studied by considering integral inequalities of disturbance quantities. In this way stability criteria and conditions for disturbance growth or decay can be derived. In pipe flow, Joseph & Carmi [10] obtained a Reynolds number 82.88 for absolute stability of a disturbance with a azimuthal periodicity of one and no streamwise variation. In flows where global properties are important for the instability like in centrifugal instabilities, the global theories are quite successful in predicting conditions for stability. In the case of plane Couette flow, the flow is shown to be nonlinearly and globally stable for all Re (Reynolds number) under the assumption of streamwise constant disturbances [11]. In shear flows local mechanisms are thought to be important and the global theories give thus rather rough bounds for stability.

1.4 Transient Algebraic Growth

Eigenvalue analysis is traditionally performed to investigate the linear stability of a given flow configuration. The least stable among the exponentially decaying eigensolutions to the linearized disturbance equations provides information about the flow behavior at large times. However, initial conditions which give transient energy growth may exist, i.e. a possibility related to the non-normality of the governing operator. *This transient energy amplification is also referred to as non-modal since it is not due to the behavior of a single eigenmode but it is caused by the superposition*

of several. In some cases the energy growth can be large enough to trigger nonlinear interactions and take the flow into a new configuration.

The initial disturbance that is able to induce the largest perturbation at a given time is called optimal and can be computed by applying optimization techniques [12].

1.4.1 Non-normal Effects

As an alternative to traditional models of instability, the significance of algebraic initial growth has recently become recognized. Algebraic growth can occur from the coalescence of eigenvalues (i.e. degeneracies) of the governing equations. The existence of degeneracies or direct resonances have potential to give an initial growth even for damped modes since they produce terms of the form $[t \cdot \exp(c_i t)]$ which may grow initially even for $c_i < 0$.

Nevertheless, the degeneracies or direct resonances are not the only mechanisms for an algebraic growth to occur in parallel shear flows. Rather algebraic growth is a general property of all parallel shear flows. Mathematically, the amplification is due to non-normal properties of the governing operators. The eigen functions of the system are then non-orthogonal. *For such systems damped eigen modes can initially cancel each other but due to different damping rates later interact to produce a large amplification decay.*

The transient growth (before final decay) of infinitesimal perturbations has generally been attributed to the existence of degenerate or nearly degenerate eigenvalues of the stability problem. It has been argued that non-normality associated to non-commutability with adjoint of linearized differential operator can be systematically responsible for the transient linear growth of disturbances. Misfit directions with respect to eigen directions can then grow, if their growth is sufficient enough, they can interact through nonlinearities and can cause a transition to new flow state.

The first indication of transient growth was found by Orr (1907) who examined two-dimensional linear Couette flow problem but the extent of transient growth was however not quantified. Algebraic growth for inviscid three-dimensional disturbances has also been demonstrated by Wilke. Landahl [13] gave a physical interpretation of no-eigenmode growth by showing that the lifting up of fluid elements in the normal direction generates streamwise velocity disturbances. This so-called lift-up mechanism is of an algebraic nature and for streamwise independent disturbances, Ellengsen & Palm [14] found an algebraic instability. For this particular type of disturbance the streamwise disturbance increases linearly with time since vertical velocity disturbance is independent of time.

In the viscous linear case, in an attempt to explain the formation of streaks in boundary layers, Hultgren & Gustavsson [15] considered the development of streamwise independent disturbances with a spanwise dependence. In this case, the vertical velocity disturbance consists solely of a Continuous spectrum which is found to have substantial amplitude inside the boundary layer in contrast to findings by Grosch & Salwen (1978) for spanwise independent disturbances. The forcing of the vertical velocity disturbance in the streamwise disturbance equation then gives an initial algebraic growth of the streamwise disturbance.

Farrell [12] examined the problem of finding the optimal transient growth for two dimensional viscous disturbances in plane Poiseuille and plane Couette flow. A rapid transient growth was found and for plane poiseuille flow the growth rates were almost two orders of magnitude larger than the growth of unstable mode at Reynolds number *10000*. Gustavsson [16] considered three dimensional initial value problem for plane poiseuille flow. A large amplification of disturbance energy was obtained at subcritical Reynolds number where only damped modes exist. The growth is substantially larger than in the two dimensional case and can be interpreted as induced by forcing the normal velocity in vertical vorticity equation (this forcing is absent in two-dimensional

case). Subsequently, Butler & Farrell [17] used a variational technique to calculate the largest possible amplification of energy for three dimensional disturbances in plane Poiseuille, Couette and Boundary layer flows. In all cases considerable amplifications were found.

Non-normal operators can conveniently be analyzed by considering the pseudospectra (Trefethen 1992) and numerical range of governing operators. For exponentially damped disturbances, transient growth is then indicated by the extent of pseudospectra and numerical range into unstable half-plane. Emanating from this concept, transient growth has been studied by Reddy, Schmid & Henningson [18]. The dependence of growth on wavenumbers, time and Reynolds number was examined and high eigenvalue sensitivity of governing operators was pointed out. In Reddy & Henningson [19] both three and two dimensional disturbances in addition to the effect of degenerate eigenvalues were investigated.

In experiments on the evolution of a localized disturbance in plane Poiseuille flow, Klingmann [20] found that transient growth occurs when the disturbance evolves. By Direct Numerical Simulations of the linearized Navier-Stokes equations, Henningson, Lundbladh & Johansson [21] found that three dimensionality allows for algebraic growth of the normal vorticity. The growth was the largest at small streamwise wave numbers and generated therefore primary streamwise elongated structures.

While the previous studies focused on the non-normality of operators and its relation to initial condition uncertainty [24], the effect of other kinds of uncertainties has not been addressed. Bobba and his coworkers [22, 23, 24] studied the effect of body forcing uncertainty, both deterministic and stochastic, in wall bounded channel flows. Various normed based measures of characterizing growth and the importance of using various other stability notions in instability studies are also addressed here.

1.5 Present Thesis

The motivation for the chosen problem is given in Chapter 2. Chapter 3 discusses the infinite domain spectral problem. Chapter 4 discusses the stability problem in the finite domain. Exact time dependent solutions are generated in Chapter 5. Comparison of linear and nonlinear results is done in Chapter 6. Finally, Conclusion and Summary of main results are presented in Chapter 7.

In this thesis we study the effect of spatial domain size, number of modes, non-hermitianness and non-normality on the transient and asymptotic stability properties of a standing, viscous compressible flow problem.

CHAPTER 2

DISSIPATING SHOCK WAVE EQUATION

2.1 Motivation

One of the motivations of this thesis is to study the domain size effects on the spectral and stability properties of the Navier-Stokes (NS) equations. Because of the complexity of the NS equations, this is a very hard question to solve. With the above limitation, we are interested in studying a simpler nonlinear partial differential equation that shares similar features to the NS equations. If this simpler PDE can be understood thoroughly, (1) we can draw approximate conclusions for the NS equations, (2) tells us what to expect in the NS equations case and (3) what kind of techniques work for the NS case.

Incompressible NS equations in 3D are governed by

$$\begin{aligned}
 \frac{\partial u_x}{\partial x} + \frac{\partial u_y}{\partial y} + \frac{\partial u_z}{\partial z} &= 0, \tag{2.1} \\
 \rho \left(\frac{\partial u_x}{\partial t} + u_x \frac{\partial u_x}{\partial x} + u_y \frac{\partial u_x}{\partial y} + u_z \frac{\partial u_x}{\partial z} \right) &= -\frac{\partial p}{\partial x} + \mu \left(\frac{\partial^2 u_x}{\partial x^2} + \frac{\partial^2 u_x}{\partial y^2} + \frac{\partial^2 u_x}{\partial z^2} \right) + f_1, \\
 \rho \left(\frac{\partial u_y}{\partial t} + u_x \frac{\partial u_y}{\partial x} + u_y \frac{\partial u_y}{\partial y} + u_z \frac{\partial u_y}{\partial z} \right) &= -\frac{\partial p}{\partial y} + \mu \left(\frac{\partial^2 u_y}{\partial x^2} + \frac{\partial^2 u_y}{\partial y^2} + \frac{\partial^2 u_y}{\partial z^2} \right) + f_2, \\
 \rho \left(\frac{\partial u_z}{\partial t} + u_x \frac{\partial u_z}{\partial x} + u_y \frac{\partial u_z}{\partial y} + u_z \frac{\partial u_z}{\partial z} \right) &= -\frac{\partial p}{\partial z} + \mu \left(\frac{\partial^2 u_z}{\partial x^2} + \frac{\partial^2 u_z}{\partial y^2} + \frac{\partial^2 u_z}{\partial z^2} \right) + f_3.
 \end{aligned}$$

Some of the key features of the above NS equations are quadratic nonlinearity, unsteadiness, and dissipation, and they interact with each other in generating complex

motions. An equation that shares many of the above features is the Burgers equation given by

$$\frac{\partial u}{\partial t} + u \frac{\partial u}{\partial x} = \nu \frac{\partial^2 u}{\partial x^2} + f(x, t), \quad (2.2)$$

where u is the velocity field and is a function of space x and time t , ν is kinematic viscosity of fluid with $\nu \geq 0$ a nominally small positive parameter, and $f(x, t)$ is the forcing function.

Burgers' equation is a quasi-linear parabolic equation introduced by J. M. Burgers [25] as a one-dimensional scalar analog for isotropic turbulence. It has been studied by many authors [25], [27], [26], [29] in different contexts, like turbulence, large eddy simulation (LES), statistical closures, numerical methods, gasdynamic shocks and others.

Burgers' equation 2.2 describes the evolution of the field $u = u(x, t)$ under non-linear advection and linear dissipation. When the viscosity ν is zero (inviscid) the field will develop a shock. For small viscosity the solution will be a slightly smoothed version of the inviscid (shock) solution. That is, sharp gradients will develop and slowly dissipate as $t \rightarrow \infty$ and the solution decays to zero. For moderate values of the viscosity the solution decays to zero and gradients do not intensify [28].

2.2 Time Independent Nonlinear Base State

The steady state Burgers' equation in the absence of forcing is

$$\frac{\partial}{\partial x} \left(\frac{1}{2} u^2(x) - \nu u_x(x) \right) = 0 \quad x \in (c, d), \quad (2.3)$$

with the dirichlet boundary conditions $u(c) = w_c > w_d = u(d)$, further solving the above equation leads to

$$\nu u_x(x) = \frac{1}{2} (u^2(x) - c_0), \quad (2.4)$$

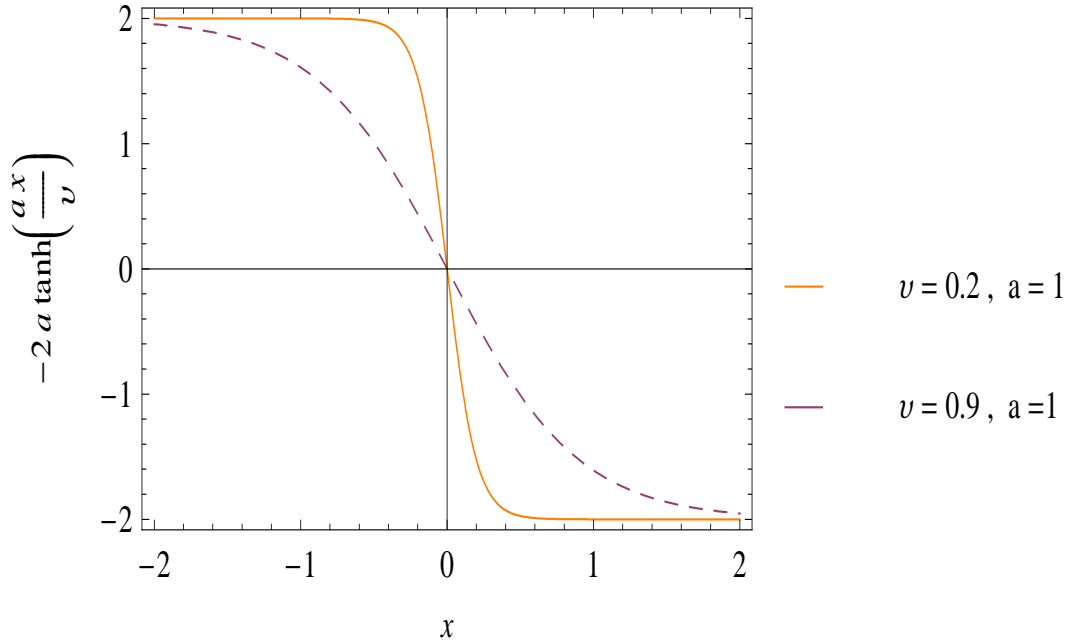


Figure 2.1. Plot of steady state solution for different viscosity values

where c_0 is a constant. Since $u(c) = w_c > w_d = u(d)$, the solution $u(\cdot)$ must decrease somewhere in the interval (c,d) and so $u(\cdot)$ must be also negative somewhere in the interval. Then (2.4) implies that c_0 must be positive, and the above equation is solved to give

$$\bar{u}(x) = -2a \tanh\left(\frac{ax}{\nu} + b\right), \quad (2.5)$$

where a and b are constants.

This hyperbolic tangent profile is nearly constant throughout the interval (c,d) with a shock located somewhere in the interior of the interval (see Figure (2.1)). The shock becomes more pronounced as ν becomes small. As the viscosity becomes large but not infinite the solution tends to be more smooth, can also be stated otherwise as, higher viscosity prevents sharp discontinuities in the solution. This property of viscosity can also be seen in real fluid problems.

CHAPTER 3

SPECTRUM OF THE DISCONTINUITY IN THE INFINITE DOMAIN

A finite dimensional differential equation $\dot{x}(t) = Ax, x \in R^n, A \in R^{n \times n}$ has finite size spectrum, of size precisely n . A partial differential equation can have countably infinite number of eigenvalues, for example, one dimensional heat equation on a finite domain $[0, L]$. By countably infinite, it means there exist a bijection between the set of natural numbers N and the set of eigenvalues. If there is no such bijection we call the set uncountably infinite. A partial differential equation can also have uncountably infinite number of eigenvalues, for example, one dimensional heat equation on the infinite domain $[0, \infty]$.

In the heat equation case, the eigenvalues are $\lambda_n = -n^2\pi^2/L^2, n \in N \cup 0$ in finite domain case with zero Dirichlet boundary conditions. The distance between two adjacent eigenvalues tends to zero as $L \rightarrow \infty$ and in the infinite domain case leads to branch cut. The branch cut is the negative real axis in the complex plane. The spectrum set in the above case fills the entire line (and hence will be called line spectrum in our terminology), is unbounded and is connected. By connected it means that one can draw a continuous line between any two eigenvalues in spectrum set and all the points on this line will also lie in the spectrum set. In this terminology, the finite size and countably infinite size spectrum's mentioned before form a disconnected set and they will be referred to as point spectrum, this also makes sense from their physical structure point of view. While the spectrum's of aforementioned shapes are well known in fluid mechanics literature, to the best of our knowledge, we're not

aware of fluid operators whose spectrum either occupies an unbounded area and is connected or is empty.

In this chapter we present two infinite dimensional fluid operators arising from 1D Burgers equation in infinite spatial domain whose spectrum is empty in one case and unbounded in another case.

3.1 Base Flow Structure

The nonlinear forced Burgers equation is given by

$$\frac{\partial u}{\partial t} + u \frac{\partial u}{\partial x} = \nu \frac{\partial^2 u}{\partial x^2} \quad x \in (-\infty, \infty). \quad (3.1)$$

From previous chapter it can be seen that

$$\bar{u}(x) = -2a \tanh\left(\frac{ax}{\nu} + b\right) \quad (3.2)$$

is a time independent nonlinear solution of (3.1). Without loss of generality, picking a co-ordinate system such that $\bar{u}(0) = 0$ and this implies $b = 0$, and hence $\bar{u}(\infty) = -2a$ and $\bar{u}(-\infty) = 2a$. As can be seen, the base state here is a smooth discontinuity at the origin of magnitude $4a$.

3.2 Forward Evolution Operator

Now we will linearize the above nonlinear equations about the base flow. Writing the velocity field as

$$u(x, t) = \bar{u}(x) + U(x, t), \quad (3.3)$$

and linearizing the Burgers equation about the steady state solution we obtain

$$\frac{\partial U}{\partial t} + \bar{u}(x) \frac{\partial U}{\partial x} + U(x, t) \frac{d\bar{u}}{dx} = \nu \frac{\partial^2 U}{\partial x^2} \quad (3.4)$$

with $U(x = \pm\infty) = 0$. This condition comes from the fact and assumption that perturbations should decay at infinity. The above equations can be written in the operator form as

$$\frac{\partial U}{\partial t} \equiv AU, \quad \text{where} \quad AU(x, t) \equiv \nu \frac{\partial^2 U}{\partial x^2} - \bar{u} \frac{\partial U}{\partial x} - \frac{d\bar{u}}{dx} U. \quad (3.5)$$

3.3 Definition of the Inner Product Space

In this thesis, we are interested in the L_2 inner product space, though the function space of Burgers equation is H_2 Banach space. We mention that the notion of adjoint depends on the choice of the inner product space and hence one has to be careful in applying the conclusions.

The spatial Lebesgue L_2 inner product is defined as

$$\langle F_1(x), F_2(x) \rangle_{L_2} = \int_{-\infty}^{\infty} F_1(x) F_2(x) dx, \quad (3.6)$$

and the adjoint operator A^* of operator A is defined using the inner product norm as

$$\langle AF_1(x), F_2(x) \rangle_{L_2} = \langle F_1(x), A^*F_2(x) \rangle_{L_2}. \quad (3.7)$$

3.4 Adjoint Evolution Operator: Non Hermitianness and Non-normality

Integrating by parts and implementing the above said Boundary conditions, the adjoint operator can be written as

$$A^*V(x, t) = \nu \frac{\partial^2 V}{\partial x^2} + \bar{u} \frac{\partial V}{\partial x} \quad \text{where} \quad V(x = \pm\infty) = 0. \quad (3.8)$$

From A and A^* it can be seen that $A \neq A^*$ and therefore A is non-Hermitian. It can also be shown after some lengthy algebra that,

$$\begin{aligned} AA^* &= \nu^2 \frac{\partial^4}{\partial x^4} + (-\bar{u}^2 + \nu \bar{u}') \frac{\partial^2}{\partial x^2} + (-2\bar{u}\bar{u}' + \nu \bar{u}'') \frac{\partial}{\partial x}, \\ A^*A &= \nu^2 \frac{\partial^4}{\partial x^4} + (-\bar{u}^2 - 2\nu \bar{u}') \frac{\partial^2}{\partial x^2} + (-\bar{u}\bar{u}' - \nu \bar{u}'') \frac{\partial}{\partial x} - \bar{u}\bar{u}'' - \nu \bar{u}''', \end{aligned}$$

where $'$ denotes d/dx . From the above it can be seen that

$$A \neq A^*, \quad (3.9)$$

$$AA^* \neq A^*A, \quad (3.10)$$

and hence A is not only *non-Hermitian* but also *non-normal* in the chosen L_2 inner product.

An interesting question is under what limits does the above equations become Hermitian and Normal? It can be seen that when base state, \bar{u} , is zero the equations are Hermitian and also Normal. On the other hand, when the base state has no shear (i.e. no spatial gradients) the operators are Normal but non-Hermitian. Obviously both these effects play a significant role at the location of the shock where they are maximum.

3.5 Non-dimensionalization

Non-dimensionalizing A and A^* , so as to write the equations in an unified way: Since there is no length scale in the problem, but there is velocity scale a . Using a and ν , one can form length scale as ν/a and time scale as a^2/ν . Denoting $s = t\nu/a^2$, $y = xa/\nu$, $M = U/a$ and $N = V/a$ we get the non-dimensional A equations as

$$\frac{\partial M}{\partial s} \equiv BM \quad \text{where} \quad M(y = \pm\infty) = 0 \quad \text{and} \quad (3.11)$$

$$BM(y, s) = \frac{\partial^2 M}{\partial y^2} + 2\tanh(y) \frac{\partial M}{\partial y} + 2\operatorname{sech}^2(y)M. \quad (3.12)$$

B is the non-dimensional form of forward operator(A). Similarly the adjoint B^* equations corresponding to A^* can be written as

$$\frac{\partial N}{\partial s} \equiv B^*N \quad \text{where} \quad N(y = \pm\infty) = 0 \quad \text{and} \quad (3.13)$$

$$B^*N(y, s) = \frac{\partial^2 N}{\partial y^2} - 2\tanh(y) \frac{\partial N}{\partial y}. \quad (3.14)$$

3.6 Point Spectrum of the Adjoint Operator

Considering the simpler adjoint equation first. Assuming that the time dependence of perturbations can be expressed in the form of $\exp(\mu t)$, the linear Initial-boundary-value problem(3.13) can be reduced to eigenvalue problem (EVP) given by

$$B^*\phi(y) = \mu\phi(y), \quad \phi(y = \pm\infty) = 0 \Rightarrow \frac{\partial^2 \phi}{\partial y^2} - 2\tanh(y) \frac{\partial \phi}{\partial y} = \mu\phi(y). \quad (3.15)$$

Where μ and ϕ are the respective eigenvalues and eigenfunctions of the Adjoint operator. The second order ordinary differential equations corresponding to EVP are solved exactly for the above.

$$\begin{aligned} \text{Let,} \quad p_1(y) &= -2 \tanh(y) \quad , \quad p_0(y) = -\mu \quad \text{and} \\ \eta(y) &= \phi(y) \exp^{\int p_1(y)/2 \, dy} = \phi(y) \operatorname{sech}(y). \end{aligned} \quad (3.16)$$

This transforms (3.13) into,

$$\eta''(y) + q_0(y)\eta(y) = 0 \quad \text{where} \quad \eta(\pm\infty) = 0 \quad (3.17)$$

$$\text{and} \quad q_0(y) = p_0 - (p_1^2/4) - (p_1'/2) = 2\text{sech}^2(y) - 1 - \mu.$$

The idea here is to generate a non-trivial solution for (3.17). And utilizing that transform the above second order equation into first order and then solve for the solutions.

Let $\eta_1(y)$ be a solution of (3.17) and the other solution is of the form

$\eta_2(y) = \eta_1(y) \int \bar{\eta}_2(y) dy$ differentiating this equation gives

$$\begin{aligned} \eta_2'(y) &= \eta_1'(y) \int \bar{\eta}_2(y) dy + \eta_1(y) \bar{\eta}_2(y) \quad \text{and} \\ \eta_2''(y) &= \eta_1''(y) \int \bar{\eta}_2(y) dy + 2\eta_1'(y) \bar{\eta}_2(y) + \eta_1(y) \bar{\eta}_2'(y). \end{aligned}$$

Substituting in (3.17) gives

$$\int \bar{\eta}_2(y) dy \left(\eta_1''(y) + \left(2\text{sech}^2(y) - 1 - \mu \right) \eta_1(y) \right) + 2\eta_1'(y) \bar{\eta}_2(y) + \eta_1(y) \bar{\eta}_2'(y) = 0$$

$$\begin{aligned} \Rightarrow 2\eta_1'(y) \bar{\eta}_2(y) + \eta_1(y) \bar{\eta}_2'(y) &= 0 \\ \Rightarrow \bar{\eta}_2(y) &= \eta_1^{-2}(y), \\ \eta_2(y) &= \eta_1(y) \int \eta_1^{-2}(y) dy. \end{aligned}$$

General solution is of the form $\eta(y) = A\eta_1(y) + B\eta_2(y)$. The only unknown here is $\eta_1(y)$. To generate a solution for $\eta_1(y)$ factorize (3.17) into the equivalent form as shown below and solving for $\eta_1(y)$ gives

$$(D + \alpha_1(y))(D + \alpha_2(y))\eta(y) = 0, \quad D = \frac{d}{dy}. \quad (3.18)$$

Assuming that the solution $\eta(y)$ is such that $(D + \alpha_2(y))\eta(y) = 0$. Expanding (3.18) gives

$$\left(D^2 + D\alpha_2(y) + \alpha_1(y)D + \alpha_1(y)\alpha_2(y) + \alpha_2'(y) \right) \eta(y) = 0$$

$$\begin{aligned}
&\Rightarrow \left(D^2\eta(y) + \underbrace{D\alpha_2(y)\eta(y)} + \alpha_1(y)D\eta(y) + \alpha_1(y)\alpha_2(y)\eta(y) + \alpha_2'(y)\eta(y) \right) = 0 \\
&\Rightarrow \left(D^2\eta(y) + \underbrace{\eta(y)D\alpha_2(y) + \alpha_2(y)D\eta(y)} + \alpha_1(y)D\eta(y) \right) + \\
&\quad (\alpha_1(y)\alpha_2(y)\eta(y) + \alpha_2'(y)\eta(y)) = 0 \\
&\Rightarrow \left(D^2 + (\alpha_1(y) + \alpha_2(y))D + \alpha_1(y)\alpha_2(y) + \alpha_2'(y) \right) \eta(y) = 0. \tag{3.19}
\end{aligned}$$

Comparing (3.17) and (3.19) and equating the coefficients gives the following

$$\begin{aligned}
\alpha_1(y) + \alpha_2(y) = 0 &\quad \Rightarrow \alpha_1(y) = -\alpha_2(y) \quad \text{and} \\
\alpha_1(y)\alpha_2(y) + \alpha_2'(y) = q_0(y) = 2\operatorname{sech}^2(y) - 1 - \mu \\
&\Rightarrow \alpha_2'(y) - \alpha_2^2(y) = 2\operatorname{sech}^2(y) - 1 - \mu. \tag{3.20}
\end{aligned}$$

With slight abuse of notation, denoting d/dy still by $'$ results in a nonlinear equation. Equation (3.20) is nonlinear and non-homogeneous, and is called the Riccati equation, being nonlinear it has many solutions. Solving the equation further for $\eta(y)$, using the transformation $\beta_2(y) = \alpha_2 - \tanh(y)$, (3.20) transforms into another form of Riccati equation

$$\beta_2' - \beta_2^2 - 2\beta_2 \tanh(y) + \mu = 0. \tag{3.21}$$

Making another transformation $\gamma_2(y) = \mu/\beta_2$ transforms (3.21) to,

$$\gamma_2' - \gamma_2^2 + 2 \tanh(y)\gamma_2 + \mu = 0. \tag{3.22}$$

An explicit solution of (3.22) is,

$$\gamma_2(y) = \tanh(y) - \sqrt{1 + \mu} \tanh\left(y\sqrt{1 + \mu}\right). \tag{3.23}$$

Substituting backwards through all the steps for the solution

$$\alpha_2(y) = \tanh(y) + \frac{\mu}{\left(\tanh(y) - \sqrt{1+\mu} \tanh\left(y\sqrt{1+\mu}\right)\right)}.$$

From (3.18) a solution of (3.17) is given by

$$(D + \alpha_2(y)) \eta(y) = 0 \Rightarrow \frac{d\eta_1(y)}{dy} + \alpha_2(y)\eta_1(y) = 0 \Rightarrow \eta_1(y) = e^{-\int \alpha_2(y) dy}.$$

Using Risch algorithm[30] η_1 is solved for as

$$\eta_1(y) = \sqrt{1+\mu} \sinh(y\sqrt{1+\mu}) - \tanh(y) \cosh(y\sqrt{1+\mu}). \quad (3.24)$$

When $\mu = 0$ the above solution becomes a trivial solution and hence this case need to be treated separately. Similarly by Risch algorithm $\eta_2(y)$ becomes

$$\eta_2(y) = \frac{1}{2\mu\sqrt{1+\mu}} [\tanh(y) \sinh(y\sqrt{1+\mu}) - \sqrt{1+\mu} \cosh(y\sqrt{1+\mu})]. \quad (3.25)$$

When $\mu = -1$ the above solution becomes indeterminate and when $\mu = 0$ it blows up, hence these cases also need to be treated separately. Therefore, when $\mu \neq 0, -1$ the general solution to (3.17) is $\eta(y) = a_1\eta_1(y) + a_2\eta_2(y)$ with a_1 and a_2 being constants.

When $\mu = 0$, (3.17) becomes $\eta''(y) + (2\operatorname{sech}^2(y) - 1)\eta = 0$, and the two independent solutions are found to be,

$$\begin{aligned} \eta_1^{(0)}(y) &= -\frac{y\operatorname{sech}(y)}{2} - \frac{\sinh(y)}{2} \quad \text{and} \\ \eta_2^{(0)}(y) &= -\operatorname{sech}(y). \end{aligned}$$

When $\mu = -1$, (3.17) becomes $\eta''(y) + 2\operatorname{sech}^2(y)\eta = 0$ and the solutions are

$$\eta_1^{(-1)}(y) = -\tanh(y) \quad \text{and} \quad \eta_2^{(-1)}(y) = 1 - y \tanh(y).$$

Combining the above results, the general solution of (3.15) is,

$$\begin{aligned}\phi(y) &= a_1\phi_1^{(b)}(y) + a_2\phi_2^{(b)}(y) \quad \text{where} \quad (3.26) \\ \phi_1^{(b)}(y) &= \cosh(y)\eta_1^{(b)}(y) \quad \text{and} \quad \phi_2^{(b)}(y) = \cosh(y)\eta_2^{(b)}(y).\end{aligned}$$

Here b is empty when $\mu \neq 0, -1$, $b = 0$ when $\mu = 0$ and $b = -1$ when $\mu = -1$. The eigenvalues and values of constants a_1 and a_2 are determined from (3.15).

When $\mu \neq 0, -1$, substituting the boundary condition $\phi(y = \pm\infty) = 0$ in (3.26), and by letting $k = \sqrt{1 + \mu}$

$$\begin{aligned}\phi(y) &= a_1 \cosh(y) (k \sinh(ky) - \tanh(y) \cosh(ky)) + \\ &\quad a_2 \cosh(y) (k \cosh(ky) - \tanh(y) \sinh(ky)).\end{aligned}$$

As $y \rightarrow \pm\infty$ in the above equation $\cosh(y) \rightarrow e^y/2$ and $\tanh(y) \rightarrow 1$,

$$\begin{aligned}\phi(\pm\infty) &= a_1(e^y/2) \left(k \left((e^{ky} - e^{-ky})/2 \right) - \left((e^{ky} + e^{-ky})/2 \right) \right) + \\ &\quad a_2(e^y/2) \left(k \left((e^{ky} + e^{-ky})/2 \right) - \left((e^{ky} - e^{-ky})/2 \right) \right), \\ &= (a_1/4) \left(k \left(e^{(k+1)y} - e^{-(k-1)y} \right) - \left(e^{(k+1)y} + e^{-(k-1)y} \right) \right) + \\ &\quad (a_2/4) \left(k \left(e^{(k+1)y} + e^{-(k-1)y} \right) - \left(e^{(k+1)y} - e^{-(k-1)y} \right) \right).\end{aligned}$$

Consider $k = a+ib$ to be a complex number, for the above boundary condition to satisfy the exponential should only have negative powers, meaning $Re[k + 1] < 0 \Rightarrow Re[\sqrt{1 + \mu} + 1] < 0$ and $Re[k - 1] > 0 \Rightarrow Re[\sqrt{1 + \mu} - 1] > 0$ i.e... $a < -1$ and $a > 1$. Obviously there is no value of μ that simultaneously satisfies the above two conditions and hence any $\mu \neq 0, -1$ is not an eigenvalue. Considering $\mu = 0 \Rightarrow a_1 = a_2 = 0$ to satisfy the boundary conditions. But for μ to be an eigenvalue,

it should have a nontrivial solution, which is not the case here hence $\mu = 0$ is not an eigenvalue. Similar thing happens when $\mu = -1$ and hence $\mu = -1$ is also not an eigenvalue. The above conditions together imply that the spectrum S_μ of B^* is **empty**, i.e.

$$S_\mu = \{ \}$$

3.7 Point Spectrum of the Forward Operator

Assuming that the time dependence of perturbations can be expressed in the form of $\exp(\lambda t)$, the linear Initial-boundary-value problem(3.11) can be reduced to eigenvalue problem (EVP) given by

$$B\psi(y) = \lambda\psi(y) \quad \text{where} \quad \psi(y = \pm\infty) = 0. \quad (3.27)$$

Where λ , ψ represent the respective eigenvalues and eigenfunctions of the forward operator. As before, solving this EVP exactly by reducing the first order differential component:

Implementing

$$r_1(y) = 2 \tanh(y) \quad \text{and} \quad r_0(y) = 2 \operatorname{sech}^2(y) - \lambda, \quad (3.28)$$

and using the transformation

$$\zeta(y) = \psi(y) \exp^{\int (r_1(y)/2) dy} = \psi(y) \cosh(y) \quad (3.29)$$

(3.11) transforms into

$$\zeta''(y) + s_0(y)\zeta(y) = 0 \quad \zeta(\pm\infty) = 0 \quad (3.30)$$

where $s_0(y) = r_0 - (r_1^2/4) - (r_1'/2) = 2 \operatorname{sech}^2(y) - 1 - \lambda$.

Comparing (3.30) with (3.17), we see that (3.30) will be same as (3.17) if λ is replaced by μ . Implying that the intermediate transformation solution is the same for adjoint and forward Operator's respectively. Hence, solving the (3.30) will result in solutions obtained as before for adjoint operator. In the case: $\lambda \neq 0, -1$

$$\begin{aligned}\zeta_1(y) &= \sqrt{1+\lambda} \sinh(y\sqrt{1+\lambda}) - \tanh(y) \cosh(y\sqrt{1+\lambda}), \\ \zeta_2(y) &= \frac{1}{2\lambda\sqrt{1+\lambda}} [\tanh(y) \sinh(y\sqrt{1+\lambda}) - \sqrt{1+\lambda} \cosh(y\sqrt{1+\lambda})].\end{aligned}$$

When $\lambda = 0$ the two independent solutions of (3.30) are

$$\zeta_1^{(0)}(y) = -\frac{y \operatorname{sech}(y)}{2} - \frac{\sinh(y)}{2} \quad \text{and} \quad \zeta_2^{(0)}(y) = -\operatorname{sech}(y).$$

When $\lambda = -1$ the solutions are

$$\zeta_1^{(-1)}(y) = -\tanh(y) \quad \text{and} \quad \zeta_2^{(-1)}(y) = 1 - y \tanh(y).$$

Combining the above results, the general solution of (3.27) is,

$$\begin{aligned}\psi(y) &= c_1 \psi_1^{(b)}(y) + c_2 \psi_2^{(b)}(y) \quad \text{where} \quad (3.31) \\ \psi_1^{(b)}(y) &= \operatorname{sech}(y) \zeta_1^{(b)}(y) \quad \text{and} \quad \psi_2^{(b)}(y) = \operatorname{sech}(y) \zeta_2^{(b)}(y).\end{aligned}$$

Here b is empty when $\lambda \neq 0, -1$, $b = 0$ when $\lambda = 0$ and $b = -1$ when $\lambda = -1$. The eigenvalues, and values of constants c_1 and c_2 are determined from the boundary conditions (3.27). In the case $\lambda \neq 0, -1$, substituting the boundary condition $\psi(y = \pm\infty) = 0$ in (3.31), with $k = \sqrt{1+\lambda}$

$$\psi(y) = a_1 \operatorname{sech}(y) (k \sinh(ky) - \tanh(y) \cosh(ky)) + a_2 \operatorname{sech}(y) (k \cosh(ky) - \tanh(y) \sinh(ky)).$$

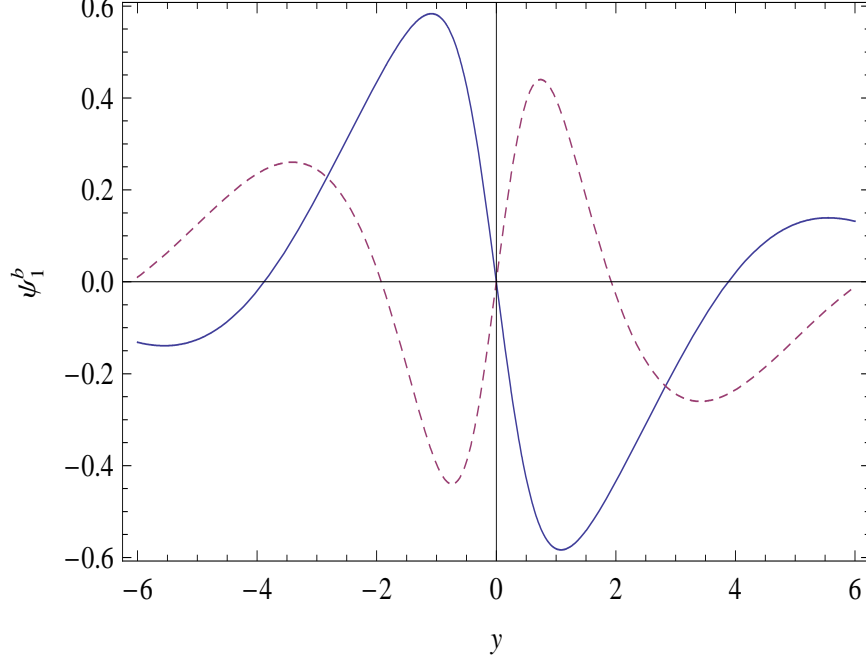


Figure 3.1. First eigenfunction $\psi_1^{(b)}(y)$ of B corresponding to $\lambda = -1 + i$. The real part is shown in solid line and the imaginary part in dashed line. Horizontal axis is the spatial co-ordinate y .

As $y \rightarrow \pm\infty$ in the above equation $\text{sech}(y) \rightarrow 2/e^y$ and $\tanh(y) \rightarrow 1$

$$\begin{aligned}
\psi(\pm\infty) &= a_1(2/e^y) \left(k \left((e^{ky} - e^{-ky})/2 \right) - \left((e^{ky} + e^{-ky})/2 \right) \right) + \\
&\quad a_2(2/e^y) \left(k \left((e^{ky} + e^{-ky})/2 \right) - \left((e^{ky} - e^{-ky})/2 \right) \right) \\
&= a_1 \left(k \left(e^{(k-1)y} - e^{-(k+1)y} \right) - \left(e^{(k-1)y} + e^{-(k+1)y} \right) \right) + \\
&\quad a_2 \left(k \left(e^{(k-1)y} + e^{-(k+1)y} \right) - \left(e^{(k-1)y} - e^{-(k+1)y} \right) \right) .
\end{aligned}$$

As before Considering $k=a+ib$ to be a complex number, for the boundary condition $\psi(\pm\infty) = 0$ to be satisfied the exponential in the above equation should have negative number in the exponent, indicating decay of eigen functions in the given domain. i.e. $\text{Re}[(k-1) < 0] \Rightarrow \text{Re}[\sqrt{1+\lambda}-1] < 0$ and $\text{Re}[(k+1) > 0] \Rightarrow \text{Re}[\sqrt{1+\lambda}+1] > 0$, leading to the relations $(a-1) < 0$ and $(a+1) > 0 \Rightarrow |a| < 1$.

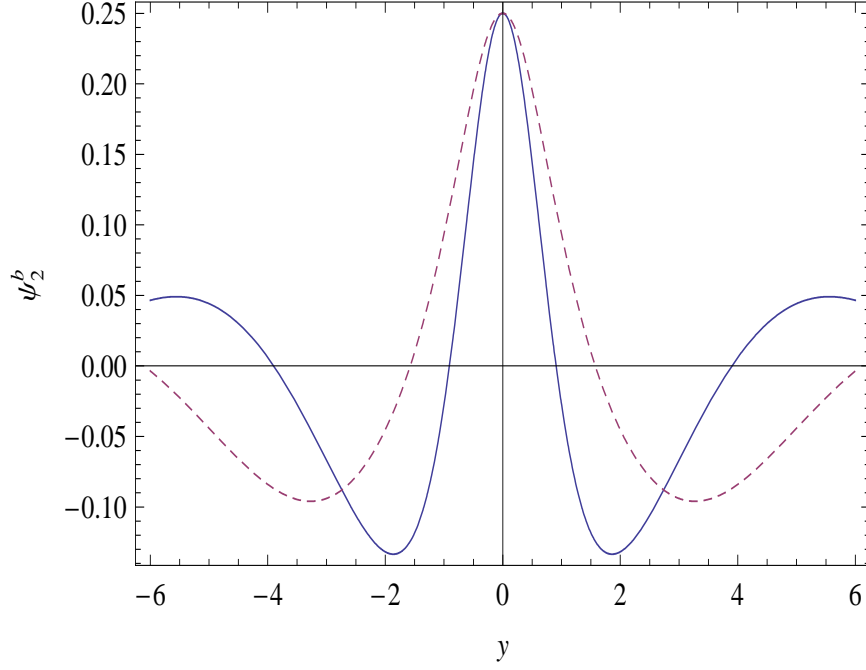


Figure 3.2. Second eigenfunction $\psi_2^{(b)}(y)$ of B corresponding to $\lambda = -1 + i$. The real part is shown in solid line and the imaginary part in dashed line. Horizontal axis is the spatial co-ordinate y .

From the λ, k relationship we have, $\lambda = k^2 - 1 = a^2 - b^2 - 1 + i(2 * a * b) \Rightarrow Re[\lambda] = (a^2 - 1) - b^2$, the term $(a^2 - 1) < 0$ already, therefore $\forall b Re[\lambda] < 0$ always. Therefore any λ such that $Re[\sqrt{1 + \lambda}] \in (-1, 1)$ is an eigenvalue of (3.27) and the corresponding eigenfunctions are $\psi_1(y, \lambda)$ and $\psi_2(y, \lambda)$. Considering $\lambda = 0$, it is understood that $a_1 = 0$ in order to satisfy the boundary conditions and hence there is only one eigenfunction $\psi_2^{(0)}(y)$ for this case. Finally when $\lambda = -1$, the boundary conditions are satisfied for any value of a_1 and a_2 , and hence there are two eigenfunctions $\psi_1^{(-1)}(y)$ and $\psi_2^{(-1)}(y)$. The above conditions together imply that the spectrum λ of B is

$$S_\lambda = \{\lambda : Re[\sqrt{1 + \lambda}] \in (-1, 1)\} \cup \{0, -1\}.$$

Since the eigenvalues λ can be complex in general, the relations between λ and $\sqrt{1+\lambda}$ can be formulated as shown below.

$$Re[\lambda] = \underbrace{(Re[\sqrt{1+\lambda}])^2}_{\mathbf{a}} - \underbrace{(Im[\sqrt{1+\lambda}])^2}_{\mathbf{b}} - 1, \quad (3.32)$$

$$Im[\lambda] = 2 \underbrace{(Re[\sqrt{1+\lambda}])}_{\mathbf{a}} \underbrace{(Im[\sqrt{1+\lambda}])}_{\mathbf{b}}. \quad (3.33)$$

For a fixed $Re[\sqrt{1+\lambda}]$, (3.32) and (3.33) are equations representing a parabola, parametrized by $Im[\sqrt{1+\lambda}]$. The boundary for the set S_λ occurs when $Re[\sqrt{1+\lambda}] = 1$ or -1 and is given by the generalized parabola $(Im[\lambda])^2 = -4Re[\lambda]$. The above boundary parabola is a limiting parabola and is not included in S_λ , however the point $0 + i0$ on the parabola is included in spectrum set S_λ .

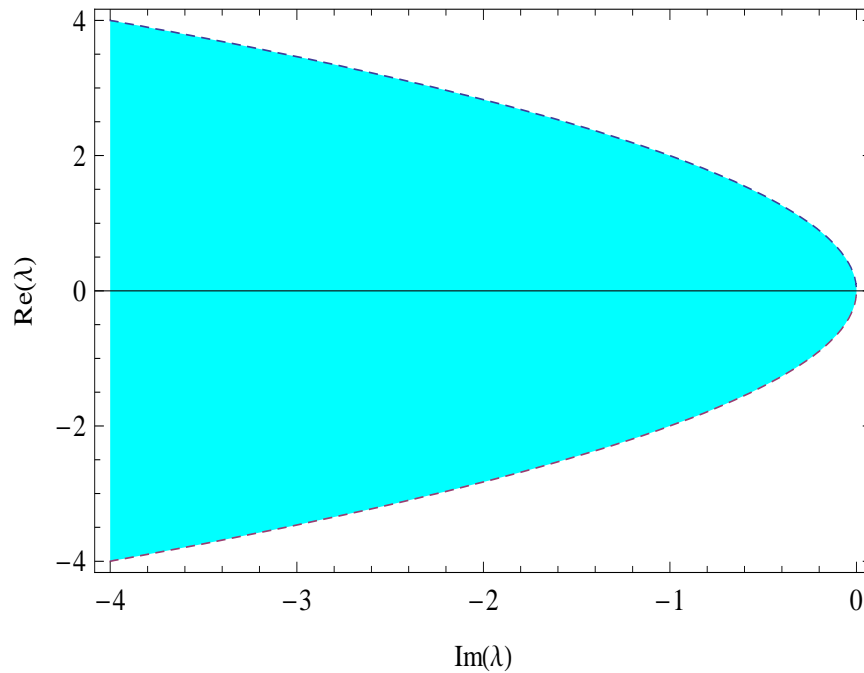


Figure 3.3. The eigenvalue spectrum of the infinite dimensional operator B in the complex plane.

As $Re[\sqrt{1+\lambda}]$ varies from -1 to 1 the spectrum sweeps an entire area. The shaded area in Figure 3.3 is the net spectrum in complex plane. The real part is shown on

horizontal axis and imaginary part on the vertical axis. From Figure 3.3, it can be seen that the spectrum of B is unbounded, is connected and fills the entire area to the left of parabola.

3.8 Spectrum Variation with Viscosity and Baseflow

The key parameters in this problem are viscosity ν and the base flow velocity a . An interesting observation and explanation of how the spectrum and eigenfunctions change as ν and a are varied is presented below.

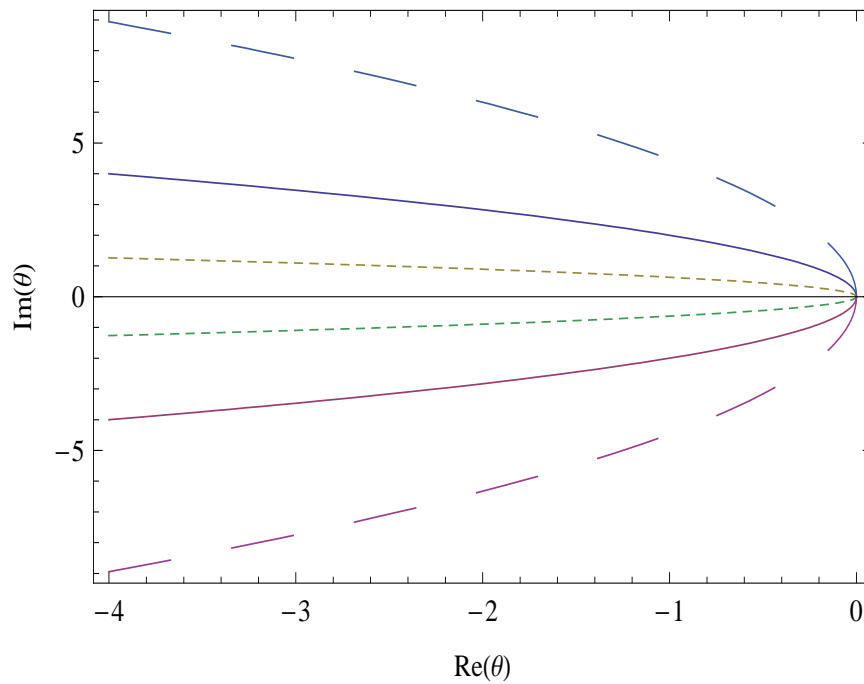


Figure 3.4. Effect of Fluid viscosity on the spectrum S_Θ in the complex plane. The area on the left of the dashed line is for $\frac{a^2}{\nu} = 5$, the area on the left of solid line is for $\frac{a^2}{\nu} = 1$, the area on the left of dotted line is for $\frac{a^2}{\nu} = 0.1$. Symmetry of each curve with $Re[\theta]$ is shown in different colors.

Since μ and λ are the eigenvalues of the nondimensional adjoint and forward operators respectively, we denote the respective eigenvalues of the dimensional operators as Δ , Θ (the associated spectrum as S_Δ and S_Θ). From the non-dimensional relations

we have $\Delta = \frac{\mu a^2}{\nu}$ and $\Theta = \frac{\lambda a^2}{\nu}$. Since increasing (or decreasing) ν with a fixed is equivalent to decreasing (or increasing) a at fixed ν . For the following, we assume that a is fixed and λ is varied. Utilizing the above facts we have the boundary set S_Θ become $(Im[\Theta])^2 = (\frac{4a^2}{\nu})Re[\Theta]$. This implies that as the viscosity decreases, the size or vertical width of the parabola grows and in the limit of zero viscosity covers almost entire left half plane. On the other hand, as viscosity increases the width of parabola decreases and in the limit of infinite viscosity S_Θ becomes negative real axis. This happens to be the spectrum of 1D Heat equation on an infinite domain, as mentioned at the beginning of this chapter. *We also point out that the parabolas right most point $(0 + i0)$ always remains the same, as viscosity is varied. The spectrum of adjoint problem S_Δ is empty.*

The above observation that the spectrum of A tends to the spectrum of the heat equation, in the limit of increasing viscosity can also be shown true with the following: From (3.5) it can be seen that as $\nu \rightarrow \infty$ i.e. as the value of ν increases we can see that forward operator $A \rightarrow \nu \frac{\partial^2}{\partial x^2}$ which is similar to the operator form of one dimensional heat equation. This can be seen as an explanation to the coincidence of the respective spectrums of forward operator and heat equation, in the limit of viscosity approaching higher values.

Similarly from (3.8), we can see that the adjoint operator $A^* \rightarrow \nu \frac{\partial^2}{\partial x^2}$ for very high values of ν (also generalized as $\nu \rightarrow \infty$). But interestingly their limit spectrums are not alike, the adjoint operator has an empty set to its spectrum and heat equation the negative real axis. Though this might look as a surprise, operators of this kind, where the limit of spectrum of operators (the adjoint operator here) is different from the spectrum of the limit operator (heat equations operator), are not uncommon in functional analysis literature.

3.9 Discussion

Two infinite dimensional operators, that arise in the context of fluid mechanics, whose spectrum is empty in one case and unbounded in another case are presented. In the unbounded case, the spectrum fills the entire area on one side of a parabola in the complex plane and is connected. The variation of the spectrum and eigenfunctions as the viscosity and eigenfunctions are varied is also presented.

To put in a larger perspective, fluid operators of the kind presented in this chapter pose several new challenges from theoretical fluid mechanics and feedback flow control standpoint. In the former case, it is not clear how techniques like eigenfunction expansion, Laplace transforms, etc. can be applied here. In the latter case, no practical controller can manipulate, or relocate open loop eigenvalues in complex plane, that many modes at the same time.

In the next chapter we consider how the spectrum and stability properties vary as the domain size is made finite in size.

CHAPTER 4

STABILITY OF THE DISCONTINUITY IN THE FINITE DOMAIN

In this chapter we will study

1. the effect of domain size on the point spectrum of Burgers equation and
2. the exponential stability behavior of the base flow state.

4.1 Linearized Forward Disturbance Equation

The afore mentioned Burgers' equation [39] in a finite domain is

$$\frac{\partial u}{\partial t} + u \frac{\partial u}{\partial x} = \nu \frac{\partial^2 u}{\partial x^2} + f(x, t) \quad \text{where } x \in (-c, c). \quad (4.1)$$

Here u is the velocity field and is a function of space x and time t , ν is kinematic viscosity of fluid with $\nu \geq 0$ and c is the domain size. The forcing term $f(x,t)$ is assumed to be zero. We have seen before that

$$\bar{u}(x) = -2a \tanh\left(\frac{ax}{\nu} + b\right) \quad (4.2)$$

is a time independent solution of (4.1).

Without loss of generality one can take $b = 0$ and in this case $\bar{u}(0) = 0$, $\bar{u}(c) = \beta$ and $\bar{u}(-c) = \alpha$, where $\alpha = -\beta$ are the boundary conditions.

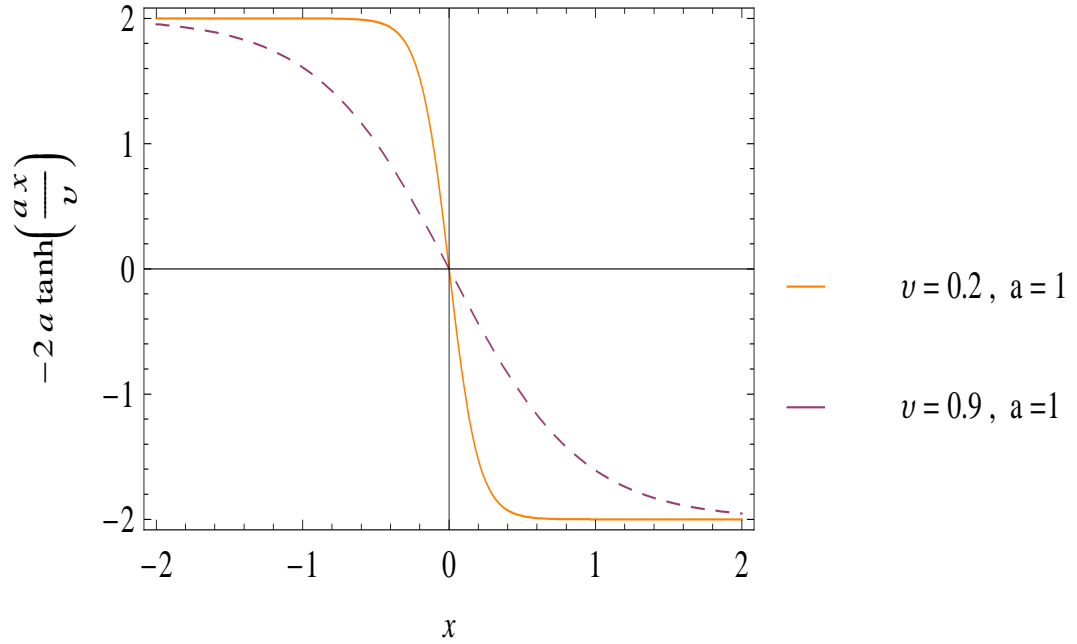


Figure 4.1. Plot of steady state solution for different viscosity values

In physical terms, this steady state can be thought of as a standing shock wave at the origin. Writing the velocity field as

$$u(x, t) = \bar{u}(x) + U(x, t) \quad (4.3)$$

and linearizing the Burgers' equation about the steady state solution gives

$$\frac{\partial U}{\partial t} + \bar{u}(x) \frac{\partial U}{\partial x} + U(x, t) \frac{d\bar{u}}{dx} = \nu \frac{\partial^2 U}{\partial x^2} \quad (4.4)$$

where $U(x = \pm c) = 0$ (assuming that the perturbations decay at the boundaries).

The above equations can be written in the operator form as

$$\frac{\partial U}{\partial t} \equiv AU \quad \text{where} \quad A \equiv \nu \frac{\partial^2}{\partial x^2} - \bar{u} \frac{\partial}{\partial x} - \frac{d\bar{u}}{dx}. \quad (4.5)$$

4.2 Adjoint Disturbance Equation

Defining the spatial L_2 inner product to be

$$\langle F_1(x), F_2(x) \rangle_{L_2} = \int_{-c}^c F_1(x) F_2(x) dx.$$

Using this, the adjoint (A^*) of operator A is defined as

$$\langle AF_1(x), F_2(x) \rangle_{L_2} = \langle F_1(x), A^*F_2(x) \rangle_{L_2}. \quad (4.6)$$

Considering the left hand side of expression initially leads to

$$\langle AF_1(x), F_2(x) \rangle_{L_2} = \int_{-c}^c \left(\nu \frac{\partial^2 F_1(x)}{\partial x^2} - \bar{u} \frac{\partial F_1(x)}{\partial x} - F_1(x) \frac{d\bar{u}}{dx} \right) F_2(x) dx.$$

Individually the above three integrands are

$$\begin{aligned} \int_{-c}^c \nu \frac{\partial^2 F_1(x)}{\partial x^2} F_2(x) dx &= \left(\nu F_2(x) \frac{\partial F_1(x)}{\partial x} \right)_{-c}^c - \int_{-c}^c \nu \frac{\partial F_2(x)}{\partial x} \frac{\partial F_1(x)}{\partial x} dx \\ &= - \left(\nu \frac{\partial F_2(x)}{\partial x} \right)_{-c}^c + \nu \int_{-c}^c \frac{\partial^2 F_1(x)}{\partial x^2} F_1(x) dx \\ &= \nu \int_{-c}^c \frac{\partial^2 F_1(x)}{\partial x^2} F_1(x) dx. \end{aligned} \quad (4.7)$$

since $F_1(\pm c) = 0$, from (4.4)

$$- \int_{-c}^c \frac{\partial \bar{u}}{\partial x} F_1(x) F_2(x) dx = - \int_{-c}^c \frac{\partial \bar{u}}{\partial x} F_2(x) F_1(x) dx. \quad (4.8)$$

$$- \int_{-c}^c \bar{u} \frac{\partial F_1(x)}{\partial x} F_2(x) dx = - (\bar{u} F_2(x) F_1(x))_{-c}^c + \int_{-c}^c F_1(x) \frac{\partial \bar{u} F_2(x)}{\partial x} dx. \quad (4.9)$$

From (4.7),(4.8) and(4.9) it is understood that there is a constitutive expression for the left hand side of expression in (4.6) which is equal to the right hand side

$$\langle F_1(x), A^*F_2(x) \rangle_{L_2} = \int_{-c}^c F_1(x) A^*F_2(x) dx.$$

Comparing the Integral terms on both right and left hand side respectively

$$\begin{aligned}
A^*F_2(x) &= \nu \frac{\partial^2 F_2(x)}{\partial x^2} - \frac{\partial \bar{u}}{\partial x} F_2(x) + \frac{\partial(\bar{u}F_2(x))}{\partial x} \\
&= \nu \frac{\partial^2 F_2(x)}{\partial x^2} - \frac{\partial \bar{u}}{\partial x} F_2(x) + \frac{\partial \bar{u}}{\partial x} F_2(x) + \bar{u} \frac{\partial F_2(x)}{\partial x} \\
&= \bar{u} \frac{\partial F_2(x)}{\partial x} + \nu \frac{\partial^2 F_2(x)}{\partial x^2}.
\end{aligned}$$

$$A^*V(x, t) = \nu \frac{\partial^2 V}{\partial x^2} + \bar{u} \frac{\partial V}{\partial x}, \quad V(x = \pm c) = 0. \quad (4.10)$$

4.3 Non-Normality and Non-Hermitian Properties

From the values of A and A^* obtained in (4.5),(4.10) it can be seen that $A \neq A^*$ and therefore A is non-Hermitian. On a side note, it can also be seen that

$$AA^* = \nu^2 \frac{\partial^4}{\partial x^4} + (-\bar{u}^2 + \nu \bar{u}') \frac{\partial^2}{\partial x^2} + (-2\bar{u}\bar{u}' + \nu \bar{u}'') \frac{\partial}{\partial x} \quad \text{and} \quad (4.11)$$

$$A^*A = \nu^2 \frac{\partial^4}{\partial x^4} + (-\bar{u}^2 - 2\nu \bar{u}') \frac{\partial^2}{\partial x^2} + (-\bar{u}\bar{u}' - \nu \bar{u}'') \frac{\partial}{\partial x} - \bar{u}\bar{u}'' - \nu \bar{u}'''. \quad (4.12)$$

Where $'$ denotes d/dx . From above we see that $AA^* \neq A^*A$ and hence A is not only non-hermitian but also non-normal in the chosen inner product.

One can see that it is only in the limit when base flow velocity $\bar{u} = 0$, that the operators $A = A^*$ and $AA^* = A^*A$, showing *hermitian* and *normal* operator behavior unlike above.

4.4 Non-Dimensionalization

Since there is no length scale in the problem, but there is velocity scale a , using a and ν , one can form length scale as ν/a and time scale as a^2/ν . Denoting $s = t\nu/a^2$, $y = xa/\nu$, $M = U/a$ and $N = V/a$ we get the non-dimensional A equation as

$$\frac{\partial M}{\partial s} \equiv BM \quad \text{where } M(y = \pm c) = 0 \quad \text{and}$$

$$BM(y, s) = \frac{\partial^2 M}{\partial y^2} + 2\tanh(y)\frac{\partial M}{\partial y} + 2\operatorname{sech}^2(y)M. \quad (4.13)$$

B is the non-dimensional A . Similarly the adjoint A^* equations become

$$\begin{aligned} \frac{\partial N}{\partial s} &\equiv B^*N \quad \text{where } N(y = \pm c) = 0 \quad \text{and} \\ B^*N(y, s) &= \frac{\partial^2 N}{\partial y^2} - 2\tanh(y)\frac{\partial N}{\partial y}. \end{aligned} \quad (4.14)$$

4.5 Eigen Spectrum of the Adjoint Operator

Considering the adjoint equation, the corresponding eigenvalue problem (EVP)(4.14) is given by

$$B^*\phi(y) = \mu\phi(y) \quad \text{where} \quad \phi(y = \pm c) = 0. \quad (4.15)$$

μ and ϕ are the corresponding eigenvalues and eigenfunctions respectively. Solving these second order ordinary differential equations corresponding to EVP exactly:

Let,

$$p_1(y) = -2\tanh(y) \quad \text{and} \quad p_0(y) = -\mu. \quad (4.16)$$

And using the transformation

$$\eta(y) = \phi(y)\exp^{\int (p_1(y)/2) dy} = \phi(y)\operatorname{sech}(y) \quad (4.17)$$

(4.14) becomes

$$\eta''(y) + q_0(y)\eta(y) = 0 \quad \text{where} \quad \eta(\pm c) = 0, \quad (4.18)$$

and $q_0(y) = p_0 - (p_1^2/4) - (p_1'/2) = 2\operatorname{sech}^2(y) - 1 - \mu$. If one of the solution $\eta_1(y)$ can be found to (4.18), the other independent solution is given by

$$\eta_2(y) = \eta_1(y) \int \eta_1^{-2}(y) dy.$$

We will generate a solution to (4.18) by factorizing it into the following form

$$\left(\frac{d}{dy} + \alpha_1(y)\right)\left(\frac{d}{dy} + \alpha_2(y)\right)\eta = 0. \quad (4.19)$$

Solving the above equation gives the following relations

$$\alpha_2'(y) - \alpha_2^2(y) = 2\operatorname{sech}^2(y) - 1 - \mu \quad (4.20)$$

and $\alpha_1 = -\alpha_2$. With slight abuse of notation, denote d/dy by still $'$. The above equation is a nonlinear non-homogeneous Riccati equation, which has many solutions owing to its nonlinearity.

Making the transformation $\beta_2(y) = \alpha_2 - \tanh(y)$, (4.20) transforms into a nonlinear Bernoulli equation

$$\beta_2' - \beta_2^2 - 2\beta_2 \tanh(y) + \mu = 0. \quad (4.21)$$

Making the transformation $\gamma_2(y) = \mu/\beta_2$, (4.21) transforms into

$$\gamma_2' - \gamma_2^2 + 2 \tanh(y)\gamma_2 + \mu = 0. \quad (4.22)$$

An explicit solution of (4.22) is given by

$$\gamma_2(y) = \tanh(y) - \sqrt{1 + \mu} \tanh\left(y\sqrt{1 + \mu}\right). \quad (4.23)$$

Substituting and solving back for the intermediate transformed solution we have

$$\alpha_2 = \tanh(y) + \frac{\mu}{\left(\tanh(y) - \sqrt{1 + \mu} \tanh\left(y\sqrt{1 + \mu}\right)\right)}.$$

From (4.19) a solution of (4.18) is given by

$$\eta_1(y) = e^{-\int \alpha_2(y) dy}. \quad (4.24)$$

Using Risch algorithm η_1 can be solved for as

$$\eta_1(y) = \sqrt{1 + \mu} \sinh(y\sqrt{1 + \mu}) - \tanh(y) \cosh(y\sqrt{1 + \mu}). \quad (4.25)$$

When $\mu = 0$ the above solution becomes a trivial solution and hence this case need to be treated separately. Similarly by Risch algorithm $\eta_2(y)$ can be solved for as

$$\eta_2(y) = \frac{1}{2\mu\sqrt{1 + \mu}} [\tanh(y) \sinh(y\sqrt{1 + \mu}) - \sqrt{1 + \mu} \cosh(y\sqrt{1 + \mu})]. \quad (4.26)$$

When $\mu = -1$ the above solution becomes trivial and hence this case also needs to be treated separately. Therefore, when $\mu \neq 0, -1$ the general solution to (4.18) is $\eta(y) = a_1\eta_1(y) + a_2\eta_2(y)$ with a_1 and a_2 being constants.

When $\mu = 0$, (4.18) becomes $\eta''(y) + (2\operatorname{sech}^2(y) - 1)\eta = 0$, and the two independent solutions are

$$\begin{aligned} \eta_1^{(0)}(y) &= -\frac{y\operatorname{sech}(y)}{2} - \frac{\sinh(y)}{2} \text{ and} \\ \eta_2^{(0)}(y) &= -\operatorname{sech}(y). \end{aligned} \quad (4.27)$$

When $\mu = -1$, (4.18) becomes $\eta''(y) + 2\operatorname{sech}^2(y)\eta = 0$, and the solutions are

$$\eta_1^{(-1)}(y) = -\tanh(y) \text{ and } \eta_2^{(-1)}(y) = 1 - y \tanh(y). \quad (4.28)$$

4.5.1 Eigen Functions of the Adjoint Operator

Combining the above results, the general solution of (4.15) are

$$\phi(y) = a_1\phi_1^{(b)}(y) + a_2\phi_2^{(b)}(y) \quad \text{where} \quad (4.29)$$

$$\phi_1^{(b)}(y) = \cosh(y)\eta_1^{(b)}(y) \quad \text{and} \quad \phi_2^{(b)}(y) = \cosh(y)\eta_2^{(b)}(y). \quad (4.30)$$

When $\mu \neq 0, -1$ b is empty, when $\mu = 0$ $b = 0$ and when $\mu = -1$ $b = -1$. The eigenvalues and corresponding values of a_1 and a_2 are determined from the boundary conditions (4.15). By considering the finite domain $(c,-c)$ to be $(-2,2)$ and substituting the boundary conditions in (4.29), the analysis can be done in the following three cases for the eigen values

Case (a) $k=\sqrt{1+\mu} = 1$ Implementing the boundary condition with $k=1$ in

$$\begin{aligned} \phi(y) = & a_1(\cosh(y))[(\sqrt{1+\mu} \sinh(y\sqrt{1+\mu}) - \tanh(y) \cosh(y\sqrt{1+\mu})) + \\ & a_2(\cosh(y))[(\frac{1}{2\mu\sqrt{1+\mu}}[\tanh(y) \sinh(y\sqrt{1+\mu}) - \sqrt{1+\mu} \cosh(y\sqrt{1+\mu})])] \end{aligned}$$

results into the following coupled set of equations

$$\begin{aligned} \phi(+y) &= a_1[\tanh(y) + \text{sech}^2(y)] + a_2[\text{sech}^2(y)] = 0 \quad \text{and} \\ \phi(-y) &= a_1[-\tanh(y) + \text{sech}^2(y)] + a_2[\text{sech}^2(y)] = 0. \end{aligned}$$

Solving the above two equations gives $a_1 = 0$ and $a_2 = 0$. Hence $k=1$ does not provide non trivial solutions for the eigen function.

Case (b) $k=\sqrt{1+\mu} = 0$ Implementing the boundary condition with $k=0$ in

$$\begin{aligned} \phi(y) = & a_1(\cosh(y))[(\sqrt{1+\mu} \sinh(y\sqrt{1+\mu}) - \tanh(y) \cosh(y\sqrt{1+\mu})) + \\ & a_2(\cosh(y))[(\frac{1}{2\mu\sqrt{1+\mu}}[\tanh(y) \sinh(y\sqrt{1+\mu}) - \sqrt{1+\mu} \cosh(y\sqrt{1+\mu})])] \end{aligned}$$

results into the following coupled set of equations

$$\phi(+y) = a_1[\text{sech}^2(y)(1 - y \tanh(y))] + a_2[-\text{sech}(y) \tanh(y)] = 0 \quad \text{and}$$

$$\phi(-y) = a_1[\operatorname{sech}^2(y)(1 - y \tanh(y))] + a_2[\operatorname{sech}(y) \tanh(y)] = 0.$$

Solving the above two equations leads to $a_1 = 0$ and $a_2 = 0$. Hence $k=0$ also does not provide *non trivial solutions* for the eigenfunctions.

Case (c) $k = \sqrt{1 + \mu} \neq 1, -1, 0$

$$\begin{aligned} \phi(y) = & a_1(\cosh(y))[(\sqrt{1 + \mu} \sinh(y\sqrt{1 + \mu}) - \tanh(y) \cosh(y\sqrt{1 + \mu}))] + \\ & a_2(\cosh(y))[(\frac{1}{2\mu\sqrt{1 + \mu}}[\tanh(y) \sinh(y\sqrt{1 + \mu}) - \sqrt{1 + \mu} \cosh(y\sqrt{1 + \mu})])] \end{aligned}$$

implementing the boundary conditions in the above equation we have

$$\begin{aligned} \phi(-2) &= a_1\phi_1(-2) + a_2\phi_2(-2) = 0 \quad \text{and} \\ \phi(2) &= a_1\phi_1(2) + a_2\phi_2(2) = 0 \end{aligned}$$

The Nontrivial solution of above equations exists if the determinant of the coefficient matrix vanishes. This condition leads to the following characteristic equation:

$$(\sqrt{1 + \mu} \tanh(y\sqrt{1 + \mu}) - \tanh(y)) * (\sqrt{1 + \mu} \coth(y\sqrt{1 + \mu}) - \tanh(y)) = 0.$$

$$\sqrt{1 + \mu} \tanh(y\sqrt{1 + \mu}) - \tanh(y) = 0 \quad \text{and} \quad (4.31)$$

$$\sqrt{1 + \mu} \coth(y\sqrt{1 + \mu}) - \tanh(y) = 0 \quad (4.32)$$

(i) Consider $k = \sqrt{1 + \mu}$ has real roots:

Evaluating (4.31) $\Rightarrow k=0, \pm\delta$ as the roots where for small values of y , $\delta \rightarrow 0$ Evaluating (4.32) $\Rightarrow k=1, -1$, but from above analysis it is understood that there is no nontrivial solution for these values of k , hence these does not represent the solution.

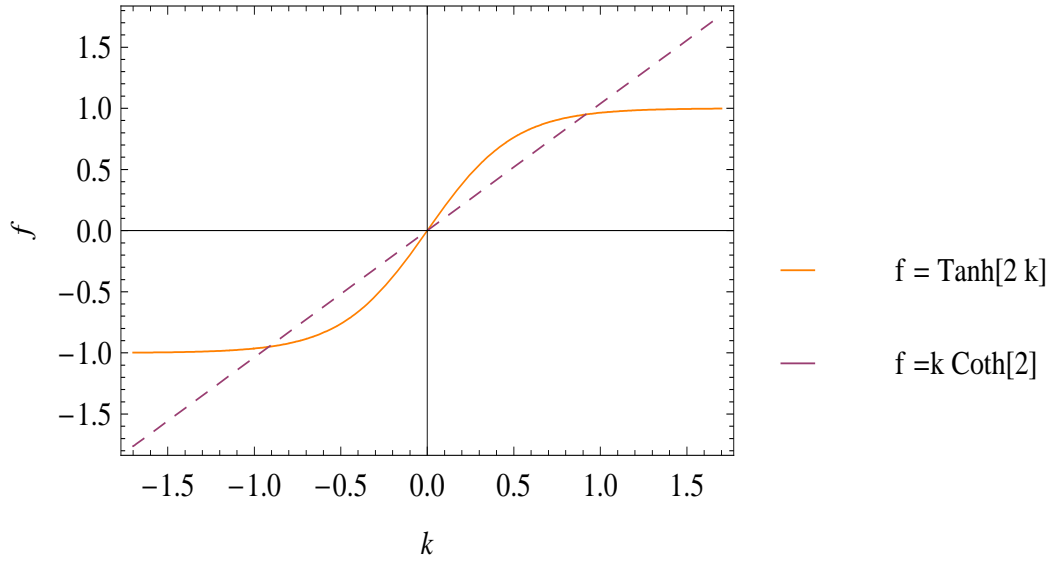


Figure 4.2. Plot showing eigenvalue μ_1 calculation for Case (c), for k_1 Real.

(ii) Consider k having purely imaginary roots i.e. $k=iz$ substituting in (4.31),(4.32) we have

$$z \tan(zy) + \tanh(y) = 0 \quad z \coth(y) - \tan(zy) = 0$$

Solving which we have $k=i1.24047$ and $k=i2.145 \dots \dots$, as shown in Figure (4.2) and Figure (4.3)

(iii) Consider k to be a complex number we have i.e... $k= p + iq$, where p is the real part and q is the complex part. Upon evaluating with the complex form of k in (4.31),(4.32) it can be seen that to have non-trivial solutions the imaginary part of k must be 0, indicating that the complex assumption reduces itself to REAL form, hence there is no k in complex form.

The eigenvalues thus obtained from the above analysis are tabulated in Table (4.1).

Since we have the eigenvalues, substituting them in (4.29) gives the individual eigenfunction explicitly as a function of non-dimensional domain length.

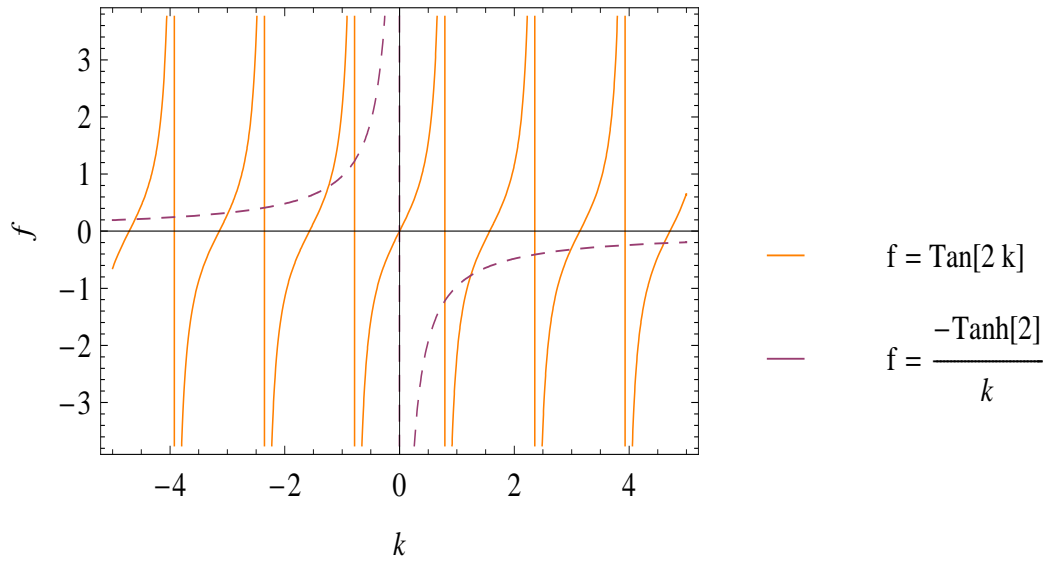


Figure 4.3. Plot showing eigenvalue's μ_2, \dots, μ_6 calculated for Case (c) with k_2, \dots, k_6 being purely complex.

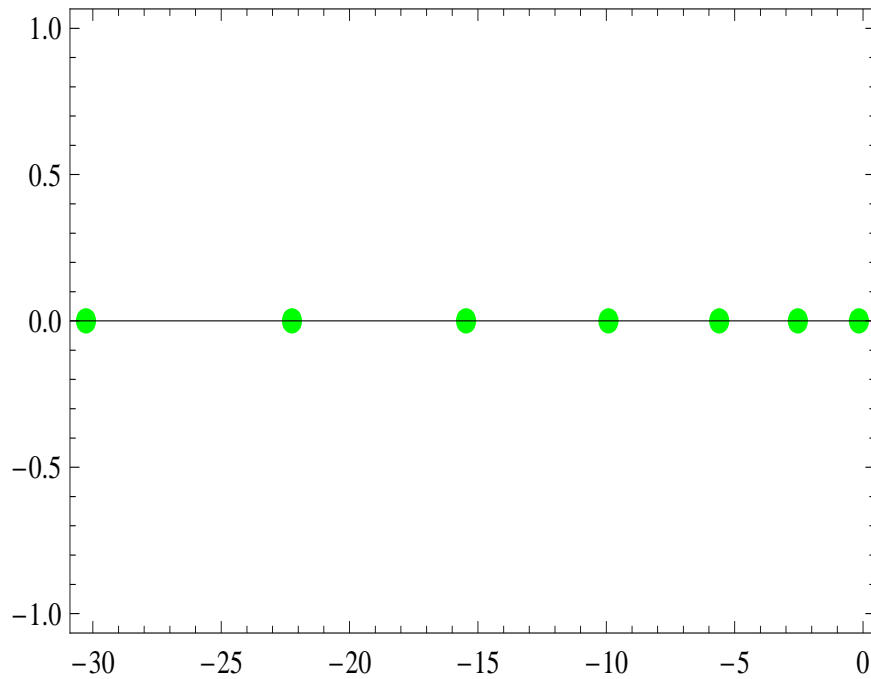


Figure 4.4. Plot of eigenvalues of the adjoint operator B^*

Table 4.1. Eigen Values of B^* in the finite domain case

Symbol	Value
μ_1	-0.16129
μ_2	-2.53877
μ_3	-5.60103
μ_4	-9.91273
μ_5	-22.24564
μ_6	-30.26388

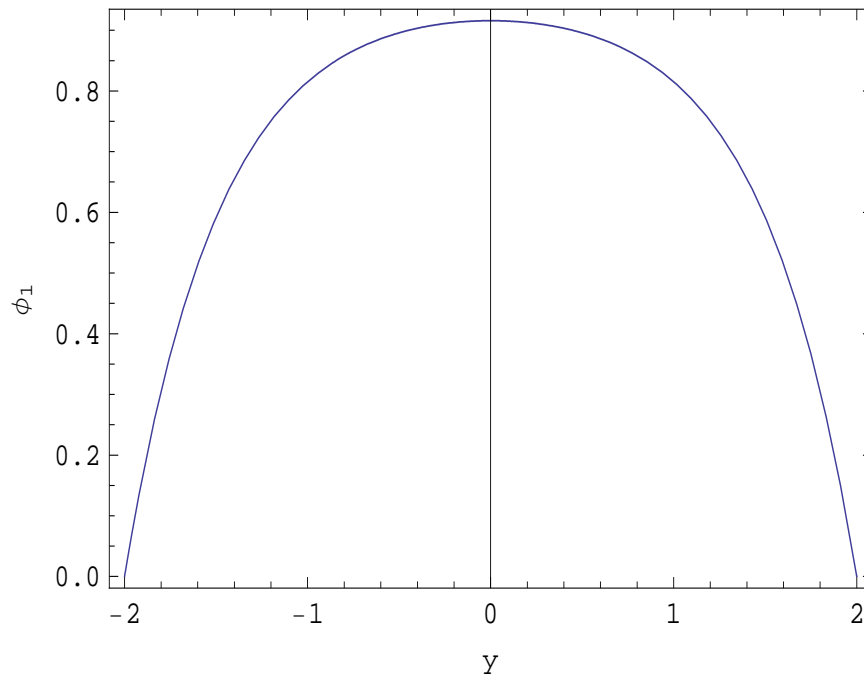


Figure 4.5. The eigenfunction of the finite dimensional operator B^* corresponding to eigenvalue μ_1

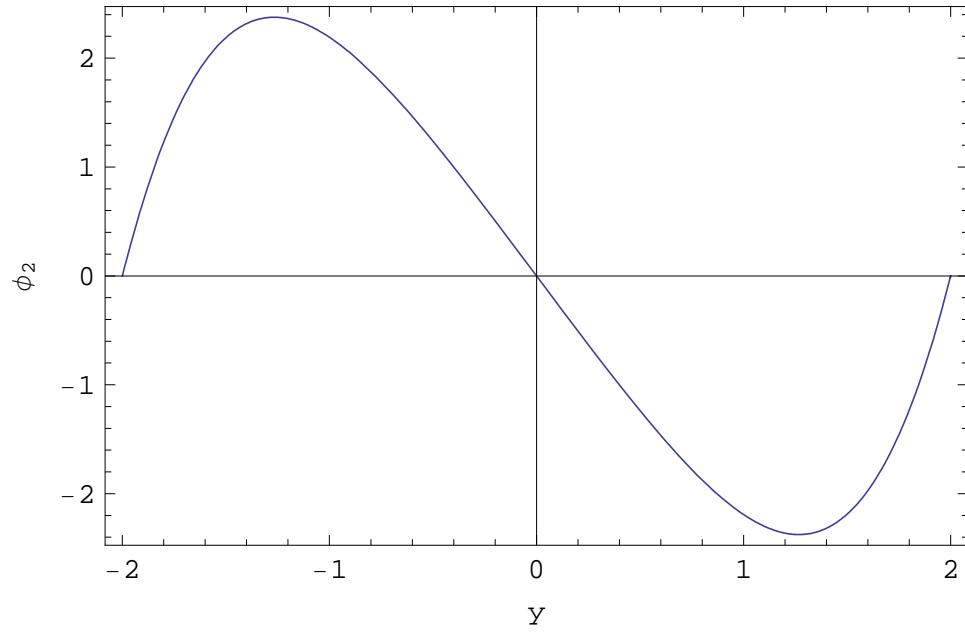


Figure 4.6. The eigenfunction of the finite dimensional operator B^* corresponding to eigenvalue μ_2

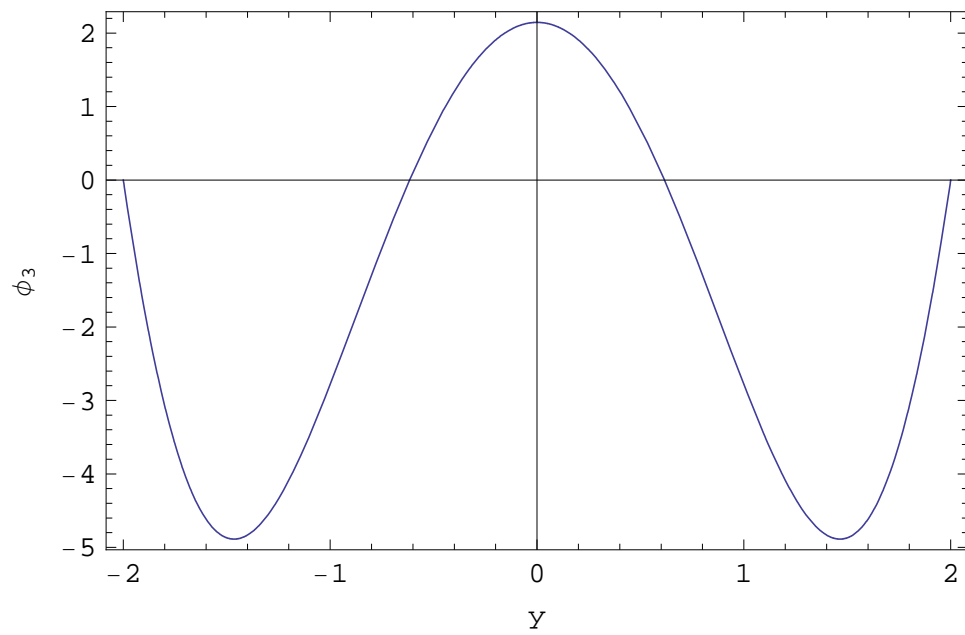


Figure 4.7. The eigenfunction of the finite dimensional operator B^* corresponding to eigenvalue μ_3

Plotting the eigenfunctions for the first three eigenvalues in Table (4.1) we have Figure (4.5), Figure (4.6) and Figure (4.7). The respective plots clearly show that the eigenfunctions are bounded and decay at boundaries. Also, Figure (4.5) and Figure (4.7) indicate that the respective eigenfunctions are symmetric with respect to vertical axis and Figure (4.6) is antisymmetric with respect to the vertical axis. This symmetric/anti-symmetric property associated with the eigenfunctions is very useful for the analysis procedures adopted in Chapter's 5 and 6.

So far, exact solution to the disturbed equation is formulated using transformations. And various possibilities that arise for solution of the equations thus obtained are postulated and solved for the eigenvalues and eigenfunctions respectively. Thus a similar procedure as followed for the adjoint operator is used to account for the eigenvalues and eigenfunctions of the forward operator in (4.13).

4.6 Eigen Spectrum for the Forward Operator

The eigenvalue problem (EVP) corresponding to (4.13) is given by

$$B\psi(y) = \lambda\psi(y) \quad \text{where} \quad \psi(y = \pm c) = 0 \quad \text{and} \quad (4.33)$$

λ , ψ are the respective eigenvalues and eigenfunctions. Next we solve this EVP exactly. Let,

$$r_1(y) = 2 \tanh(y) \quad \text{and} \quad r_0(y) = 2 \operatorname{sech}^2(y) - \lambda.$$

Using the transformation

$$\zeta(y) = \psi(y) \exp^{\int (r_1(y)/2) dy} = \psi(y) \cosh(y) \quad (4.34)$$

(4.13) transforms into the following second order differential equation

$$\zeta''(y) + s_0(y)\zeta(y) = 0 \quad \text{where} \quad \zeta(\pm\infty) = 0 \quad \text{and} \quad (4.35)$$

$$s_0(y) = r_0 - (r_1^2/4) - (r_1'/2) = 2\text{sech}^2(y) - 1 - \lambda.$$

Comparing (4.35) with (4.18), shows that (4.35) is same as (4.18) if λ is replaced by μ . Hence, following the steps as before in §3.7 for the solution of intermediate transformation we have:

when $\lambda \neq 0, -1$

$$\begin{aligned} \zeta_1(y) &= \sqrt{1+\lambda} \sinh(y\sqrt{1+\lambda}) - \tanh(y) \cosh(y\sqrt{1+\lambda}) \quad \text{and} \\ \zeta_2(y) &= \frac{1}{2\lambda\sqrt{1+\lambda}} [\tanh(y) \sinh(y\sqrt{1+\lambda}) - \sqrt{1+\lambda} \cosh(y\sqrt{1+\lambda})] \end{aligned}$$

When $\lambda = 0$, the two independent solutions of (4.35) are

$$\begin{aligned} \zeta_1^{(0)}(y) &= -\frac{y\text{sech}(y)}{2} - \frac{\sinh(y)}{2} \quad \text{and} \\ \zeta_2^{(0)}(y) &= -\text{sech}(y). \end{aligned}$$

When $\lambda = -1$, the solutions are

$$\zeta_1^{(-1)}(y) = -\tanh(y) \quad \text{and} \quad \zeta_2^{(-1)}(y) = 1 - y \tanh(y).$$

4.6.1 Eigen Functions of the Forward Operator B

Combining the above results, the general solution of (4.33) is

$$\begin{aligned} \psi(y) &= c_1\psi_1^{(b)}(y) + c_2\psi_2^{(b)}(y) \quad \text{where} \quad (4.36) \\ \psi_1^{(b)}(y) &= \text{sech}(y)\zeta_1^{(b)}(y) \quad \text{and} \quad \psi_2^{(b)}(y) = \text{sech}(y)\zeta_2^{(b)}(y). \end{aligned}$$

When $\lambda \neq 0, -1$ b is empty, when $\lambda = 0$ $b = 0$ and when $\lambda = -1$ $b = -1$. The eigenvalues, and values of c_1 and c_2 are determined from the boundary conditions

(4.33). By considering the finite domain (c,-c) to be (-2,2) and substituting the boundary conditions in (4.29)

Case (a) $k=\sqrt{1+\lambda}=1$, Implementing the boundary condition with $k=1$ in

$$\psi(y) = a_1(\cosh(y))[(\sqrt{1+\lambda} \sinh(y\sqrt{1+\lambda}) - \tanh(y) \cosh(y\sqrt{1+\lambda})) + a_2(\cosh(y))[(\frac{1}{2\mu\sqrt{1+\lambda}})[\tanh(y) \sinh(y\sqrt{1+\lambda}) - \sqrt{1+\lambda} \cosh(y\sqrt{1+\lambda})]]$$

leads to the following set of coupled equations

$$\begin{aligned}\psi(+y) &= a_1[\tanh(y) + \operatorname{sech}^2(y)] + a_2[\operatorname{sech}^2(y)] = 0 \quad \text{and} \\ \psi(-y) &= a_1[-\tanh(y) + \operatorname{sech}^2(y)] + a_2[\operatorname{sech}^2(y)] = 0.\end{aligned}$$

Solving the above two equations $\Rightarrow a_1 = 0$ and $a_2 = 0$. Hence $k=\sqrt{1+\lambda}=1$ does not provide *non trivial solutions* for the eigenfunction.

Case (b) $k=0$ Implementing the boundary condition with $k=\sqrt{1+\lambda}=0$ in

$$\psi(y) = a_1(\cosh(y))[(\sqrt{1+\lambda} \sinh(y\sqrt{1+\lambda}) - \tanh(y) \cosh(y\sqrt{1+\lambda})) + a_2(\cosh(y))[(\frac{1}{2\lambda\sqrt{1+\lambda}})[\tanh(y) \sinh(y\sqrt{1+\lambda}) - \sqrt{1+\lambda} \cosh(y\sqrt{1+\lambda})]]$$

gives the following coupled set of equations

$$\begin{aligned}\psi(+y) &= a_1[\operatorname{sech}^2(y)(1 - y \tanh(y))] + a_2[-\operatorname{sech}(y) \tanh(y)] = 0 \quad \text{and} \\ \psi(-y) &= a_1[\operatorname{sech}^2(y)(1 - y \tanh(y))] + a_2[\operatorname{sech}(y) \tanh(y)] = 0.\end{aligned}$$

Solving the above two equations $\Rightarrow a_1 = 0$ and $a_2 = 0$. Hence $k=0$ also does not provide non trivial solutions for the eigenfunction.

Case (c) $k=\sqrt{1+\lambda} \neq 1, -1, 0$

$$\begin{aligned} \psi(y) = & a_1(\cosh(y))[(\sqrt{1+\lambda} \sinh(y\sqrt{1+\lambda}) - \tanh(y) \cosh(y\sqrt{1+\lambda}))] + \\ & a_2(\cosh(y))[(\frac{1}{2\lambda\sqrt{1+\lambda}}[\tanh(y) \sinh(y\sqrt{1+\lambda}) - \sqrt{1+\lambda} \cosh(y\sqrt{1+\lambda})]] \end{aligned} \quad (4.37)$$

Implementing the boundary conditions as before gives the following set of equations

$$\begin{aligned} \psi(-2) &= a_1\psi_1(-2) + a_2\psi_2(-2) = 0 \quad \text{and} \\ \psi(2) &= a_1\psi_1(2) + a_2\psi_2(2) = 0. \end{aligned}$$

The Nontrivial solution of above equations exists if the determinant of the coefficient matrix vanishes. This condition leads to the following characteristic equations:

$$(\sqrt{1+\lambda} \tanh(y\sqrt{1+\lambda}) - \tanh(y)) * (\sqrt{1+\lambda} \coth(y\sqrt{1+\lambda}) - \tanh(y)) = 0$$

$$\sqrt{1+\lambda} \tanh(y\sqrt{1+\lambda}) - \tanh(y) = 0 \quad \text{and} \quad (4.38)$$

$$\sqrt{1+\lambda} \coth(y\sqrt{1+\lambda}) - \tanh(y) = 0. \quad (4.39)$$

(i) Considering the case that k has real roots:

Evaluating (4.38) we have $k=0, \pm\delta$ as the roots where for small values of y , $\delta \rightarrow 0$

Evaluating (4.39) we have $k=1, -1$, but from above analysis it is understood that there is no *nontrivial solution* for these values of k , hence these does not represent the solution.

(ii) Considering k having imaginary roots i.e. $k=iz$ substituting in (4.38),(4.39) leads to the following condition

$$z \tan(zy) + \tanh(y) = 0 \quad , \quad z \coth(y) - \tan(zy) = 0$$

Table 4.2. Eigen Values of B in the finite domain case

Symbol	Value
λ_1	-0.16129
λ_2	-2.53877
λ_3	-5.60103
λ_4	-9.91273
λ_5	-22.24564
λ_6	-30.26388

upon solving for k results in $k = i1.24047$ and $k = i2.145 \dots$, as shown in Figure (4.2) and Figure (4.3)

(iii) Considering k to be a complex number we have i.e.. $k = p + iq$, where p -the real part and q -the complex part. Upon evaluating with the complex form of k in (4.38),(4.39)

$$\begin{aligned} \tanh(kL) &= \frac{1}{k} \tanh(L) \\ \Rightarrow \frac{e^{(p+iq)L} - e^{-(p+iq)L}}{e^{(p+iq)L} + e^{-(p+iq)L}} &= \frac{1}{p+iq} \tanh(L) \\ \Rightarrow (p+iq) \left(e^p \cos(q) + ie^p \sin(q) - e^{-p} \cos(q) + ie^{-p} \sin(q) \right) &= \\ \tanh(L) \left(e^p \cos(q) + ie^p \sin(q) + e^{-p} \cos(q) - ie^{-p} \sin(q) \right) & \end{aligned}$$

Individually separating and equating the Real and Imaginary parts of the above equation and solving for p and q results in $p \rightarrow 0$ always $\Rightarrow k = 0 + iq$, i.e. it moves to the *purely complex regime* as described above in (ii). This result clearly indicates that there is no complex eigen value existing for the problem.

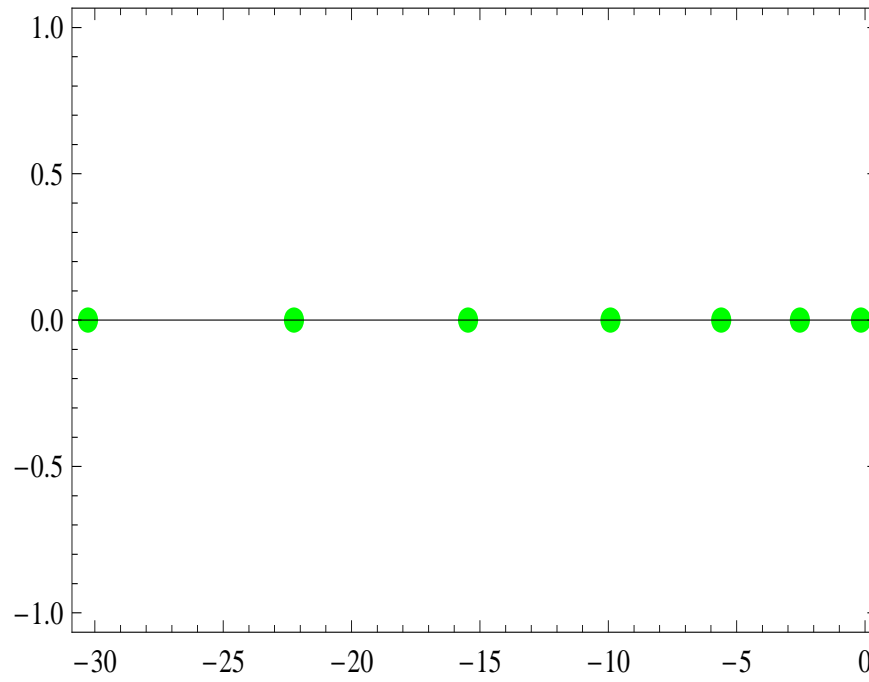


Figure 4.8. Plot of the eigenvalues of the forward operator B

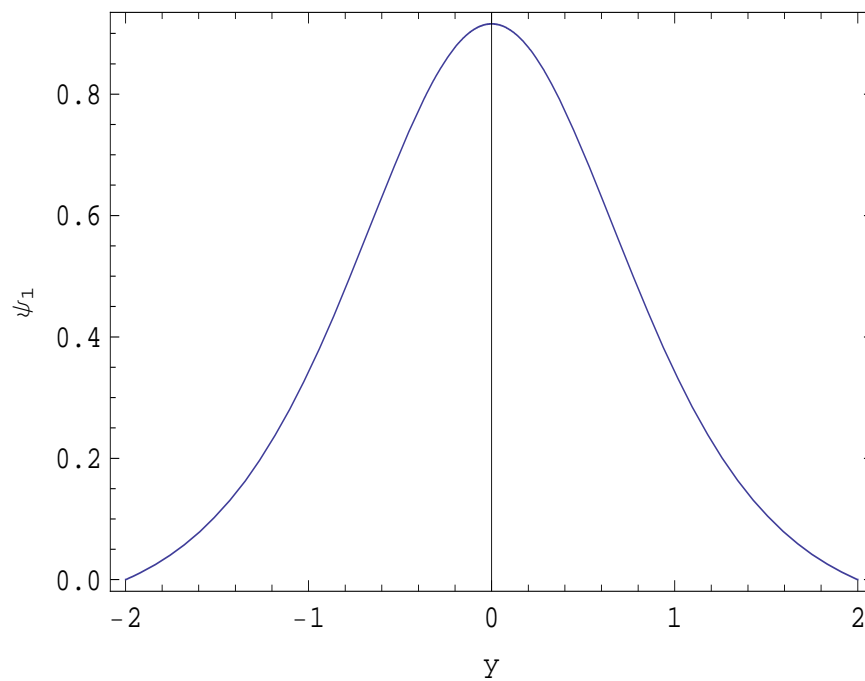


Figure 4.9. The eigenfunction of the finite dimensional operator B corresponding to the eigenvalue λ_1

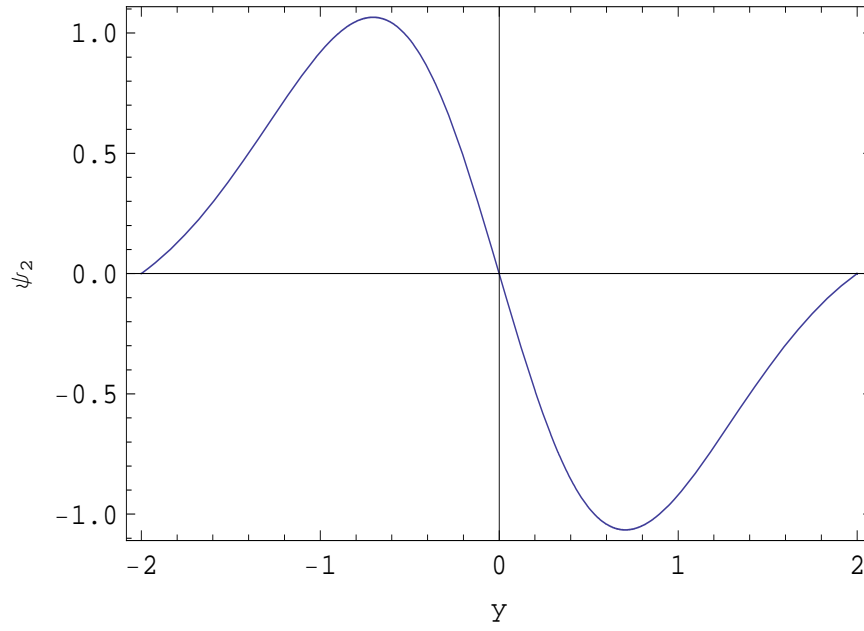


Figure 4.10. The eigenfunction of the finite dimensional operator B corresponding to the eigenvalue λ_2

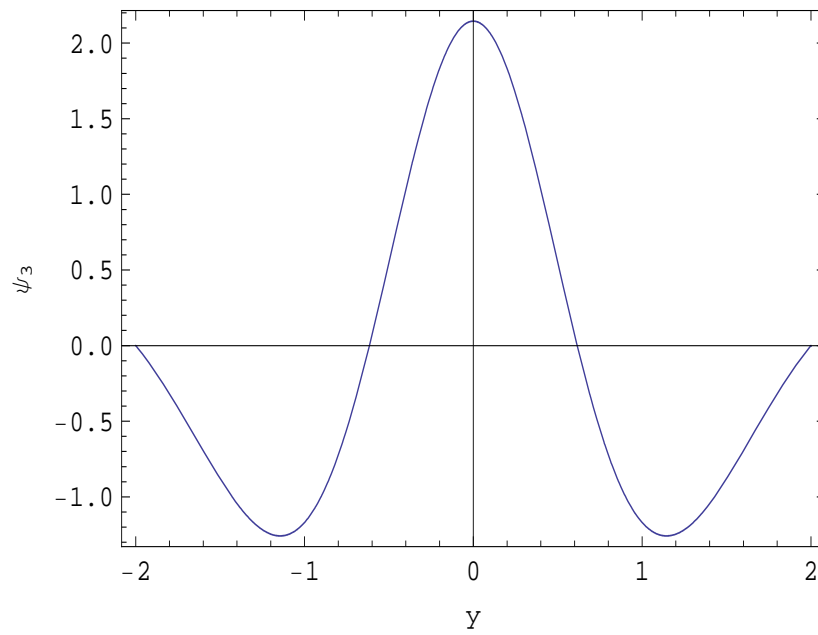


Figure 4.11. The eigenfunction of the finite dimensional operator B corresponding to the eigen value λ_3

4.7 Discussion

In this chapter we studied the spectral properties of the linearized Burgers equation on a finite spatial domain. An interesting observation is that the change of domain size dramatically alters the spectrum of the operators, comparing with infinite domain results of previous chapter. It was found that both the forward and adjoint operators have the same eigenvalues (all lie on open Left Half Plane (LHP)), but different eigenfunctions. Since all the eigenvalues are in open LHP, both the forward and adjoint operators are exponentially stable.

CHAPTER 5

EXACT SOLUTIONS USING BI-ORTHOGONAL BASIS FUNCTIONS

In this chapter, we will generate exact solution for the forward partial differential equation using a Galerkin like method, using bi-orthogonal basis functions.

5.1 Orthogonality and Bi-orthogonality

Orthogonality for an inner product space V with basis elements x_i is defined by

$$\langle x_i, x_j \rangle = \delta_{ij} \begin{cases} 1 & \text{for } i = j, \\ 0 & \text{for } i \neq j. \end{cases} \quad (5.1)$$

Note that without loss of generality we assumed that the basis elements are of unit length (or orthonormal). If this is not so, one can always normalize them.

Bi-orthogonality is a property relating two different vector spaces and it's respective basis elements. Mathematically it is stated as, for some given vector spaces X and Y with basis elements x_i and y_i respectively, are said to be bi-orthogonal if

$$\langle x_i, y_j \rangle = \delta_{ij} \begin{cases} 1 & \text{for } i = j, \\ 0 & \text{for } i \neq j. \end{cases} \quad (5.2)$$

It can be shown that the eigenfunctions of the forward and adjoint operators form a bi-orthogonal basis, i.e., $\langle \psi_n, \phi_m \rangle = a_n \delta_{nm}$, where a_n is some constant. With some abuse of notation, we assume that there is no summation over n in the above equation.

Normalizing eigenfunction ψ_i using the L_2 norm gives,

$$\int_{-c}^c \psi_i(y)\bar{\psi}_i(y) dy = b_i, \quad \psi_i^n(y) = (1/\sqrt{b_i})\psi_i(y) \quad \text{where } i = 1, 2, 3.$$

The normalized eigenfunctions are denoted by the superscript n . Some of ψ_i are purely imaginary, for example $\phi_3(y)$ eigen function corresponding the third eigen value. Multiplying an eigenfunction by a constant does not change its properties, as a result we take define $\psi_i = \psi_i/I$ in these cases. Here $I = \sqrt{-1}$.

Now we normalize ϕ_i such that the bi-orthogonal relation $\langle \psi_n^n, \phi_m^n \rangle = \delta_{nm}$. Since $\langle \psi_n^n, \phi_m \rangle = c_n \delta_{nm}$, we get this by defining $\phi_i^n \equiv \phi_i^n/c_i$.

From now on we assume that the eigenfunctions have been normalized and do not explicitly show the superscript n .

5.2 Solution of the Linear Equations

Since the eigenvectors of B form a *bi-orthogonal* set with respect to the eigenvectors of B^* , that is $\langle \psi_n, \phi_m \rangle = \delta_{nm}$, we will utilize this property to solve the linear equations exactly.

Consider the nondimensional operator equation

$$\frac{\partial M(y, s)}{\partial s} = B \times M(y, s). \quad (5.3)$$

Any solution can be represented as a superposition of the eigenfunctions as

$$M(y, s) \approx \sum_{i=1}^{i=N} p_i(s)\psi_i(y). \quad (5.4)$$

Here N can be ∞ or a finite number, if we are doing an approximation. Substituting (5.4) in (5.3) gives

$$\sum_{i=1}^{i=N} \dot{p}_i \psi_i = \left(\sum_{i=1}^{i=N} B p_i \psi_i \right) = \sum_{i=1}^{i=N} p_i \lambda_i \psi_i.$$

Taking innerproduct with respect to ϕ_j to the above equation results in the following equations

$$\begin{aligned}
\dot{p}_1 + 0 + 0 + \dots &= p_1\lambda_1 + 0 + 0 + \dots, \\
0 + \dot{p}_2 + 0 + \dots &= 0 + p_2\lambda_2 + 0 + \dots, \\
0 + 0 + \dot{p}_3 + \dots &= 0 + 0 + p_3\lambda_3 + \dots, \\
&\dots \\
0 + 0 + \dots + \dot{p}_N &= 0 + 0 + \dots + p_N\lambda_N
\end{aligned} \tag{5.5}$$

From (5.5) we get

$$\begin{aligned}
p_1(s) &= e^{\lambda_1 s} p_{10}, \quad p_2(s) = e^{\lambda_2 s} p_{20}, \quad p_3(s) = e^{\lambda_3 s} p_{30}, \dots \\
M(y, s) &= e^{\lambda_1 s} p_{10} \psi_1 + e^{\lambda_2 s} p_{20} \psi_2 + e^{\lambda_3 s} p_{30} \psi_3 + \dots, \\
M_0(x) &= M_{10} \psi_1 + M_{20} \psi_2 + M_{30} \psi_3 + \dots,
\end{aligned}$$

where $\langle M_0, \phi_1 \rangle = p_{10}$, $\langle M_0, \phi_2 \rangle = p_{20}$, $\langle M_0, \phi_3 \rangle = p_{30}$...

Using the above results, we finally get the semigroup representation of disturbance velocity as

$$M(y, s) = e^{\lambda_1 s} \langle M_0(y), \phi_1 \rangle \psi_1 + e^{\lambda_2 s} \langle M_0(y), \phi_2 \rangle \psi_2 + \dots = \sum_{i=1}^N e^{\lambda_i t} \langle M_0(y), \phi_i \rangle \psi_i.$$

5.3 Numerical Simulations: Effect of the Number of Modes and the Initial Conditions on the Transient Growth

We define the energy norm as

$$\begin{aligned}
E(s) &= \|M(y, s)\|_{L_2}^2 dx = \frac{1}{2} \langle M, M \rangle_{L_2} = \int_{-c}^c M^2 dy \\
&= \langle p_1 \psi_1 + p_2 \psi_2 + \dots, p_1 \psi_1 + p_2 \psi_2 + \dots \rangle
\end{aligned}$$

$$= \int_{-c}^c (p_1\psi_1 + p_2\psi_2 + \dots)^2 dy.$$

In this section, we consider the effect of number of retained modes and the initial conditions on the transient growth properties of the equations. To illustrate the ideas we consider $N = 2$ and $N = 3$ cases.

Case 1: N=2

The two mode approximation gives

$$\begin{aligned} E(t) &= \frac{1}{2} \langle p_1\psi_1 + p_2\psi_2, p_1\psi_1 + p_2\psi_2 \rangle \\ E(t) &= \frac{1}{2} (p_1^2 + p_2^2 + 2p_1p_2 \langle \psi_1\psi_2 \rangle) \\ E(t) &= \frac{1}{2} (e^{2\lambda_1 s} p_{10}^2 + e^{2\lambda_2 s} p_{20}^2). \end{aligned}$$

Since ψ_1 and ψ_2 are symmetric and anti-symmetric functions, as shown before, their inner product will be zero. Thus, leaving two terms which continuously decay exponentially, since the eigenvalues are in open LHP. Hence for two retained modes there can be no transient growth of the energy.

Case 2: N=3

The three mode approximation gives

$$\begin{aligned} E(t) &= \frac{1}{2} \langle p_1\psi_1 + p_2\psi_2 + p_3\psi_3, p_1\psi_1 + p_2\psi_2 + p_3\psi_3 \rangle \\ E(t) &= \frac{1}{2} \int (p_1\psi_1 + p_2\psi_2 + p_3\psi_3)^2 dy \\ E(t) &= \frac{1}{2} \left(\underbrace{e^{2\lambda_1 s} p_{10}^2}_a + \underbrace{e^{2\lambda_2 s} p_{20}^2}_b + \underbrace{e^{2\lambda_3 s} p_{30}^2}_c + \underbrace{2a_{10}a_{30} \langle \psi_1, \psi_3 \rangle e^{(\lambda_1 + \lambda_3)s}}_d \right) \quad (5.6) \end{aligned}$$

Since ψ_1 and ψ_3 are symmetric and ψ_2 is anti-symmetric the inner product of ψ_2 with ψ_1 and ψ_3 is zero, leaving behind a coupling term (shown above as d). It is this term

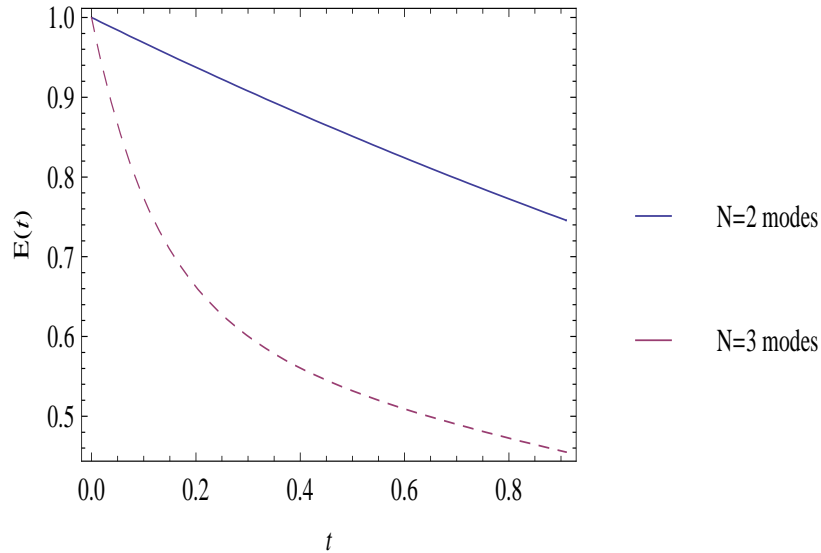


Figure 5.1. Plot of energy variation with time. Solid line represents N=2 modes and dashed line represents N=3 modes. For a specific notation we observe that in both the above cases energy decreases monotonically

that causes the transient growth. Since all the eigen values of the system are in the open left half plane, each of the above term decays exponentially, however the sum of these terms can grow transiently, if right initial conditions are available.

Next we show few illustrative simulations. Here $\langle \psi_1, \psi_3 \rangle = \beta > 0$.

Case A: Here we take $p_{1_0} = 0.2$, $p_{2_0} = 0$ and $p_{3_0} = 0.1$. The energy variation for the two and three mode cases is shown in Figure (5.1) for the above initial conditions. Note that for these initial conditions, both the two and three mode energies decay monotonically and there is no transient growth.

Case B: Here we take $p_{1_0} = 0.2$, $p_{2_0} = 0$ and $p_{3_0} = -0.1$. Figure (5.2) shows the energy variation for the two and three mode cases with the above initial conditions. Note that for these initial conditions, the two mode case energy decays monotonically, while the three mode energy first decays, then grows and finally decays.

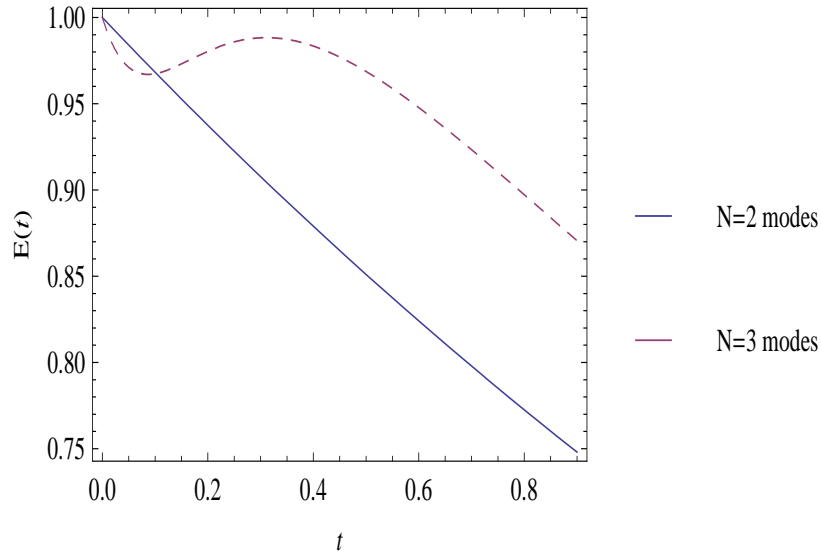


Figure 5.2. Plot of energy variation with time. Solid line represents N=2 modes and dashed line represents N=3 modes. For a specific notation we observe that, while the energy of 2 modes decreases monotonically, and that of three mode system grows transiently

From the above results, we can see that for transient growth not only non-normality, but also right number of modes and initial conditions play key roles. The above simulations were performed in Mathematica [40].

5.4 Discussion

In this chapter we solved the linearized shock problem exactly using bi-orthogonal basis functions and used it to study the energy growth and decay properties of the solutions. It was observed that non-orthogonal superposition of potentially decaying solutions can give rise to short term growth (see Figure (5.2)). It was shown that the linearized problem can exhibit large transient growths given the right initial conditions. The *source* of this transient amplification of initial conditions lies in the non-orthogonality of the eigenfunction basis. Further it was also observed that the number of modes retained plays a significant role in predicting transient growth.

CHAPTER 6

NON-LINEAR FINITE AMPLITUDE EFFECTS

In the previous chapter, we studied the dynamics neglecting the nonlinearity. In this chapter, we study the finite amplitude effects, i.e., nonlinear effects for large perturbations.

The nonlinear governing equations are given by

$$\frac{\partial M(y, s)}{\partial s} + \mathbf{B}M + \mathcal{N}(M) = 0, \quad (6.1)$$

$$\mathcal{N}(M) = M \frac{\partial M}{\partial y}. \quad (6.2)$$

6.1 Projection of the Equations on to a Finite Dimensional Space

In this section we project the above equations onto a finite dimensional subspace spanned by the first N eigenfunctions, and this is written as

$$M(y, s) = p_1(s)\psi_1(y) + p_2\psi_2 + p_3\psi_3 + \dots + p_N\psi_N. \quad (6.3)$$

Substituting the above equations in (6.1) we get

$$\sum_{i=1}^{i=N} \dot{p}_i \psi_i = \left(\sum_{i=1}^{i=N} B p_i \psi_i \right) + \mathcal{N}_i(M) = \sum_{i=1}^{i=N} p_i \lambda_i \psi_i + \mathcal{N}_i(M),$$

where

$$\mathcal{N}_i(M) = \langle \mathcal{N}(M), \phi_i \rangle, \quad (6.4)$$

$$\mathcal{N}(M) \approx \left(\sum_{i=1}^{i=N} p_i \psi_i \right) \left(\sum_{i=1}^{i=N} p_i \psi'_i \right). \quad (6.5)$$

6.2 Three Mode Subspace

To compare with the results of previous chapter, we project the nonlinear equations on to a three dimensional space. The equations in this case are:

$$\dot{p}_1 = p_1 \lambda_1 + \mathcal{N}_1(M) \quad \mathcal{N}_1(M) = \langle \mathcal{N}(M), \phi_1 \rangle, \quad (6.6)$$

$$\dot{p}_2 = p_2 \lambda_2 + \mathcal{N}_2(M) \quad \mathcal{N}_2(M) = \langle \mathcal{N}(M), \phi_2 \rangle, \quad (6.7)$$

$$\dot{p}_3 = p_3 \lambda_3 + \mathcal{N}_3(M) \quad \mathcal{N}_3(M) = \langle \mathcal{N}(M), \phi_3 \rangle, \quad (6.8)$$

and

$$\mathcal{N}(M) = (p_1 \psi_1 + p_2 \psi_2 + p_3 \psi_3) (p_1 \psi'_1 + p_2 \psi'_2 + p_3 \psi'_3).$$

Substituting the above equation in (6.6), (6.7), (6.8) we get

$$\begin{aligned} \mathcal{N}_1(M) = & p_1^2 \underbrace{\langle \psi_1 \psi'_1, \phi_1 \rangle}_{\delta_{111}} + p_2^2 \underbrace{\langle \psi_2 \psi'_2, \phi_1 \rangle}_{\delta_{221}} + p_3^2 \underbrace{\langle \psi_3 \psi'_3, \phi_1 \rangle}_{\delta_{331}} + \\ & p_1 p_2 \left[\underbrace{\langle \psi_1 \psi'_2, \phi_1 \rangle}_{\delta_{121}} + \underbrace{\langle \psi_2 \psi'_1, \phi_1 \rangle}_{\delta_{211}} \right] + p_1 p_3 \left[\underbrace{\langle \psi_1 \psi'_3, \phi_1 \rangle}_{\delta_{131}} + \underbrace{\langle \psi_3 \psi'_1, \phi_1 \rangle}_{\delta_{311}} \right] + \\ & p_2 p_3 \left[\underbrace{\langle \psi_3 \psi'_2, \phi_1 \rangle}_{\delta_{321}} + \underbrace{\langle \psi_2 \psi'_3, \phi_1 \rangle}_{\delta_{231}} \right]. \end{aligned}$$

Similarly it can be shown that

$$\begin{aligned} \mathcal{N}_2(M) = & p_1^2 \underbrace{\langle \psi_1 \psi'_1, \phi_2 \rangle}_{\gamma_{112}} + p_2^2 \underbrace{\langle \psi_2 \psi'_2, \phi_2 \rangle}_{\gamma_{222}} + p_3^2 \underbrace{\langle \psi_3 \psi'_3, \phi_2 \rangle}_{\gamma_{332}} + \\ & p_1 p_2 \left[\underbrace{\langle \psi_1 \psi'_2, \phi_2 \rangle}_{\gamma_{122}} + \underbrace{\langle \psi_2 \psi'_1, \phi_2 \rangle}_{\gamma_{212}} \right] + p_1 p_3 \left[\underbrace{\langle \psi_1 \psi'_3, \phi_2 \rangle}_{\gamma_{132}} + \underbrace{\langle \psi_3 \psi'_1, \phi_2 \rangle}_{\gamma_{321}} \right] + \\ & p_2 p_3 \left[\underbrace{\langle \psi_3 \psi'_2, \phi_2 \rangle}_{\gamma_{322}} + \underbrace{\langle \psi_2 \psi'_3, \phi_2 \rangle}_{\gamma_{232}} \right]. \end{aligned}$$

Table 6.1. Numerically computed values of γ_{ijk}

$\gamma_{111} = 0$	$\gamma_{112} = 1.175$	$\gamma_{113} = 0$
$\gamma_{221} = 0$	$\gamma_{222} = 1.50765$	$\gamma_{223} = 0$
$\gamma_{331} = 0$	$\gamma_{332} = 3.478$	$\gamma_{333} = 0$
$\gamma_{121} = -0.171054$	$\gamma_{122} = 0$	$\gamma_{123} = -6.04825$
$\gamma_{331} = 0.479$	$\gamma_{232} = 0$	$\gamma_{233} = 4.497$
$\gamma_{131} = 0$	$\gamma_{132} = 3.04632$	$\gamma_{133} = 0$

$$\begin{aligned}
 \text{and } \mathcal{N}_3(M) = & p_1^2 \underbrace{\langle \psi_1 \psi'_1, \phi_3 \rangle}_{\gamma_{113}} + p_2^2 \underbrace{\langle \psi_2 \psi'_2, \phi_3 \rangle}_{\gamma_{223}} + p_3^2 \underbrace{\langle \psi_3 \psi'_3, \phi_3 \rangle}_{\gamma_{333}} + \\
 & p_1 p_2 \left[\underbrace{\langle \psi_1 \psi'_2, \phi_3 \rangle}_{\gamma_{123}} + \underbrace{\langle \psi_2 \psi'_1, \phi_3 \rangle}_{\gamma_{213}} \right] + p_1 p_3 \left[\underbrace{\langle \psi_1 \psi'_3, \phi_3 \rangle}_{\gamma_{133}} + \underbrace{\langle \psi_3 \psi'_1, \phi_3 \rangle}_{\gamma_{313}} \right] + \\
 & p_2 p_3 \left[\underbrace{\langle \psi_3 \psi'_2, \phi_3 \rangle}_{\gamma_{323}} + \underbrace{\langle \psi_2 \psi'_3, \phi_3 \rangle}_{\gamma_{233}} \right].
 \end{aligned}$$

The values of γ_{ijk} are computed numerically and are tabulated in Table (6.1).

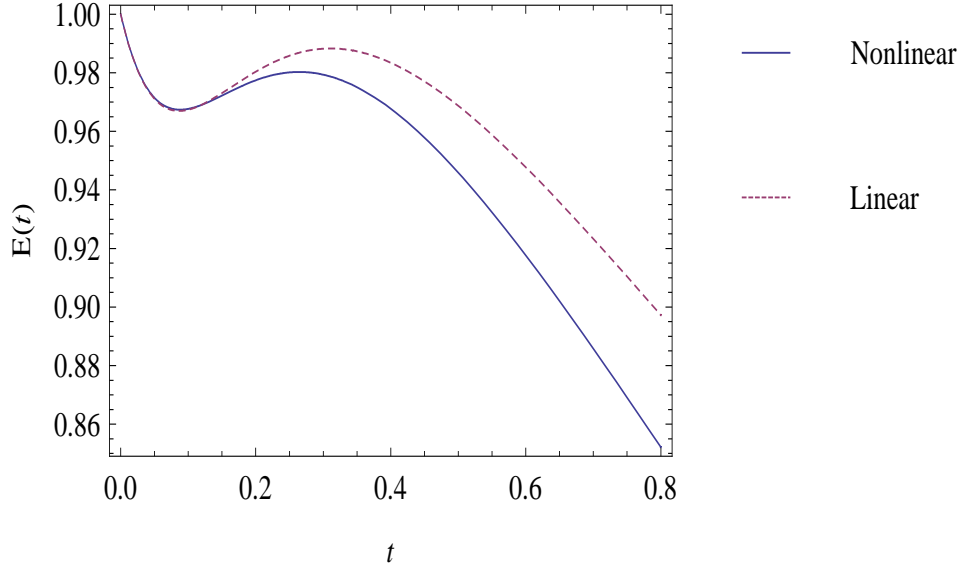


Figure 6.1. Energy variation with time for linear and nonlinear governing equations. The initial condition for the simulations are $p_{1_0} = 2.6, p_{2_0} = 0, p_{3_0} = -1.3$

6.3 Comparison of Linear and Nonlinear Energy Growth

In this section we compare the linear and nonlinear energy growth rates. The above nonlinear equations are solved numerically using an adaptive Runge Kutta method.

Figures (6.1) and (6.2) show the plot of energy variation, linear and nonlinear, for two different initial conditions. It can be seen from these figures that the linear and nonlinear results are almost same for small times. In Figure (6.2) the linear and nonlinear results deviate only by a small amount for large times, and in Figure (6.1) they deviate by a large amount. From the above results it can be seen that it is hard to predict exactly when the difference between linear and nonlinear results will be substantial. This is related to basin of attraction of the underlying fixed points and it is hard to calculate these for partial differential equations. Obviously these results have important implications for Direct Numerical Simulations (DNS) of turbulent flows.

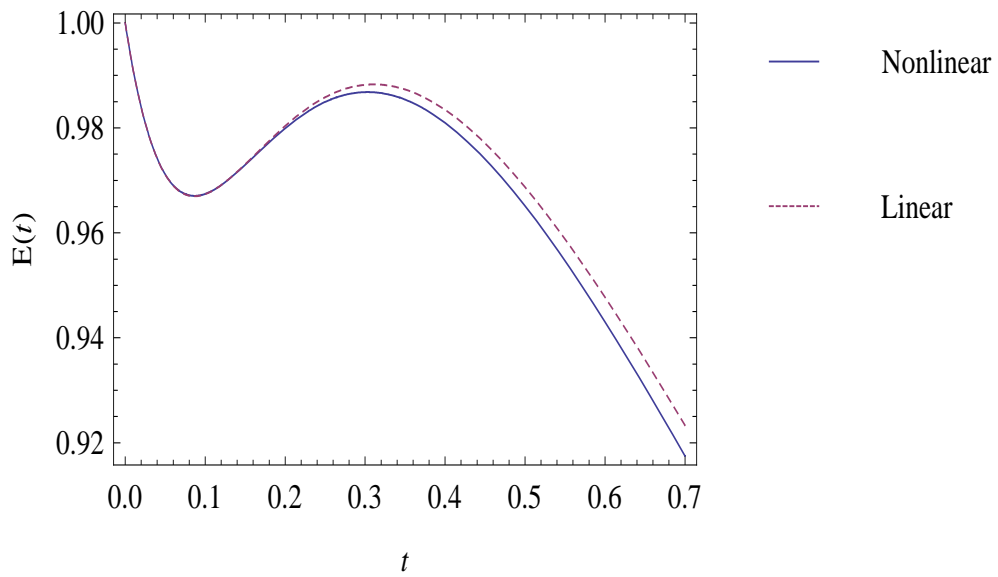


Figure 6.2. Energy variation with time for linear and nonlinear governing equations. The initial condition for the simulations are $p_{1_0} = 1.0, p_{2_0} = 0, p_{3_0} = -0.5$

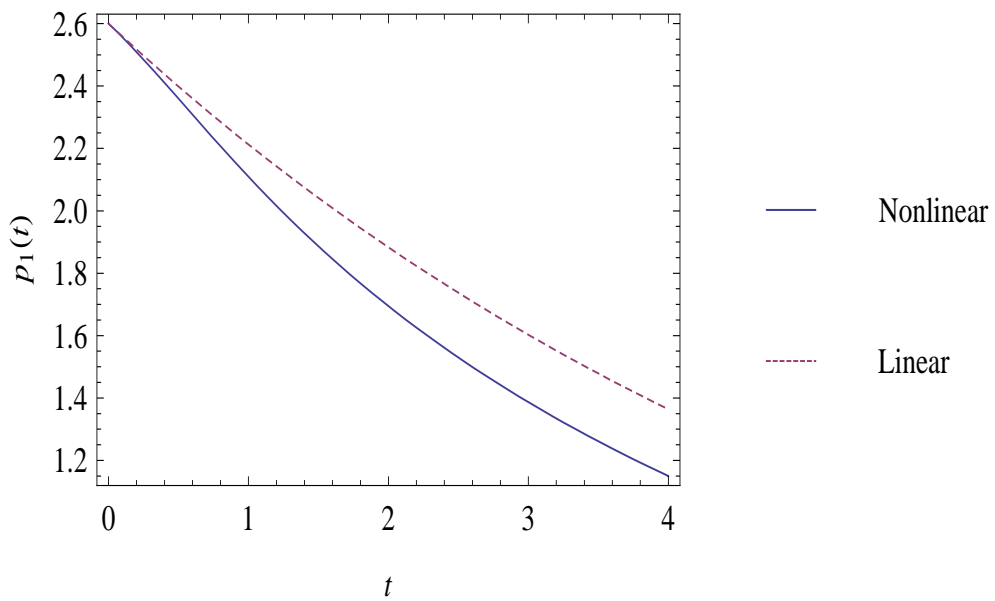


Figure 6.3. Variation of $p_1(t)$ coefficient in the linear and nonlinear simulations of Figure (6.1)

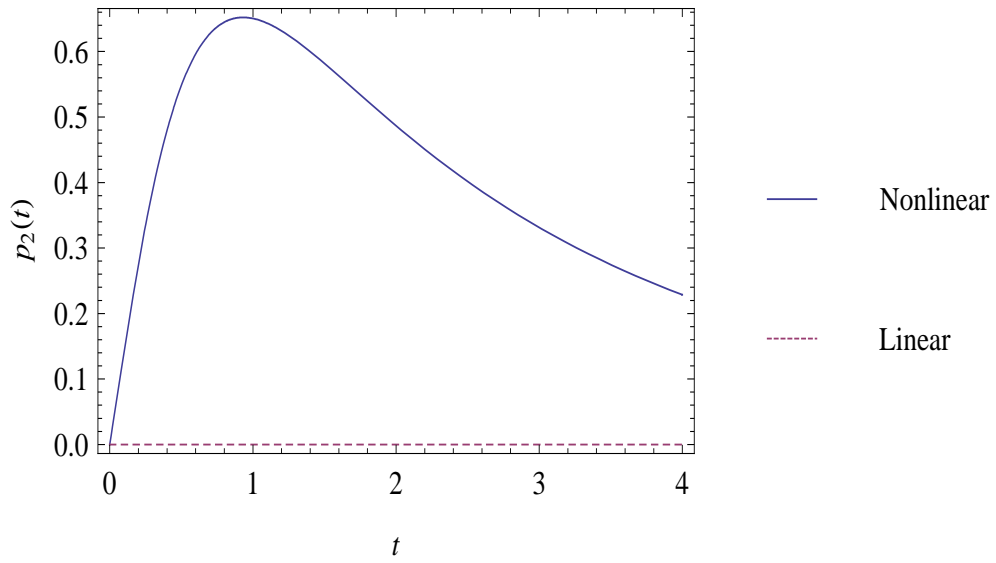


Figure 6.4. Variation of $p_2(t)$ coefficient in the linear and nonlinear simulations of Figure (6.1). Notice that the IC for $p_2[t]$ is zero and hence remains at zero in the linear case as the system is diagonal and decoupled.

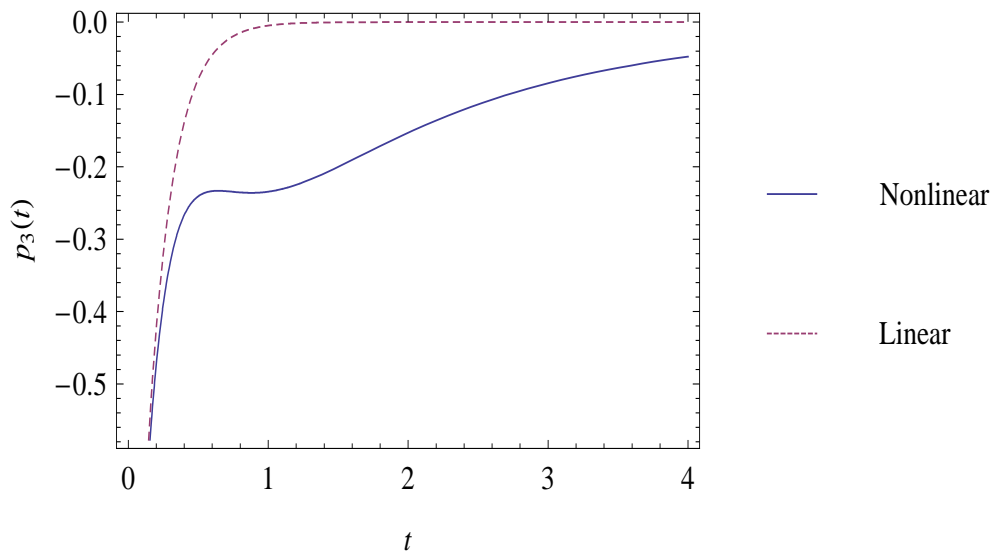


Figure 6.5. Variation of $p_3(t)$ coefficient in the linear and nonlinear simulations of Figure (6.1)

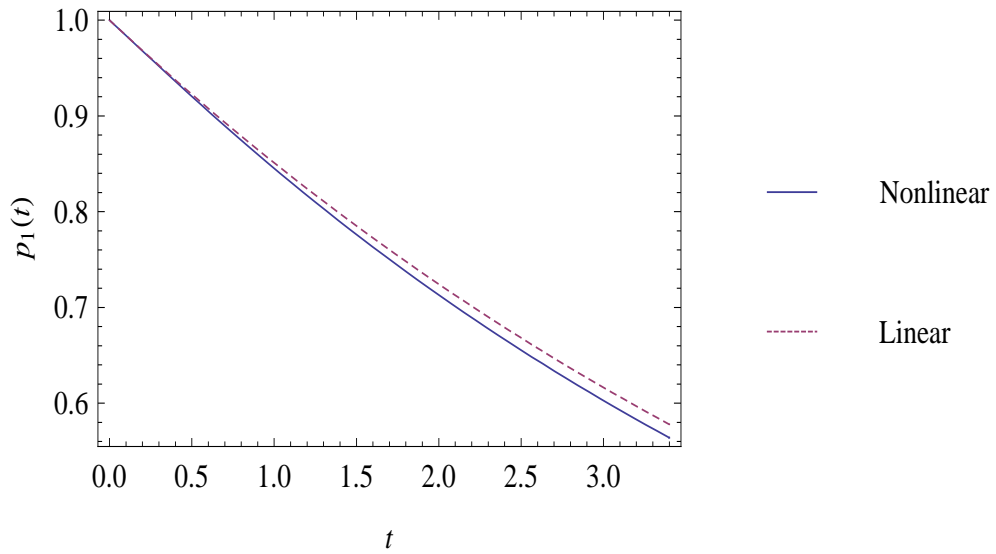


Figure 6.6. Variation of $p_1(t)$ coefficient in the linear and nonlinear simulations of Figure (6.2)

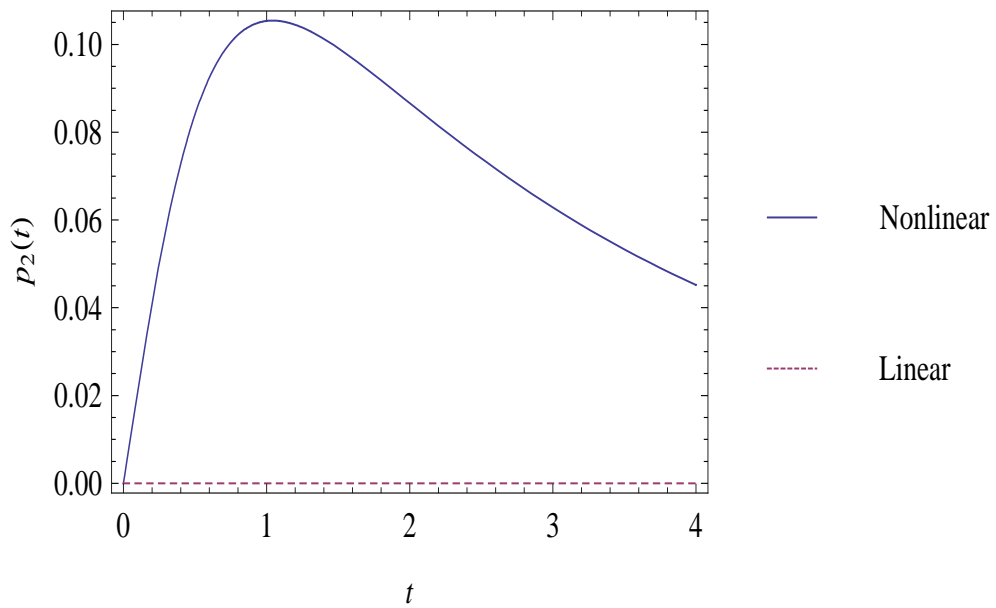


Figure 6.7. Variation of $p_2(t)$ coefficient in the linear and nonlinear simulations of Figure (6.2). Notice that the IC for $p_2[t]$ is zero and hence remains at zero in the linear case as the system is diagonal and decoupled.

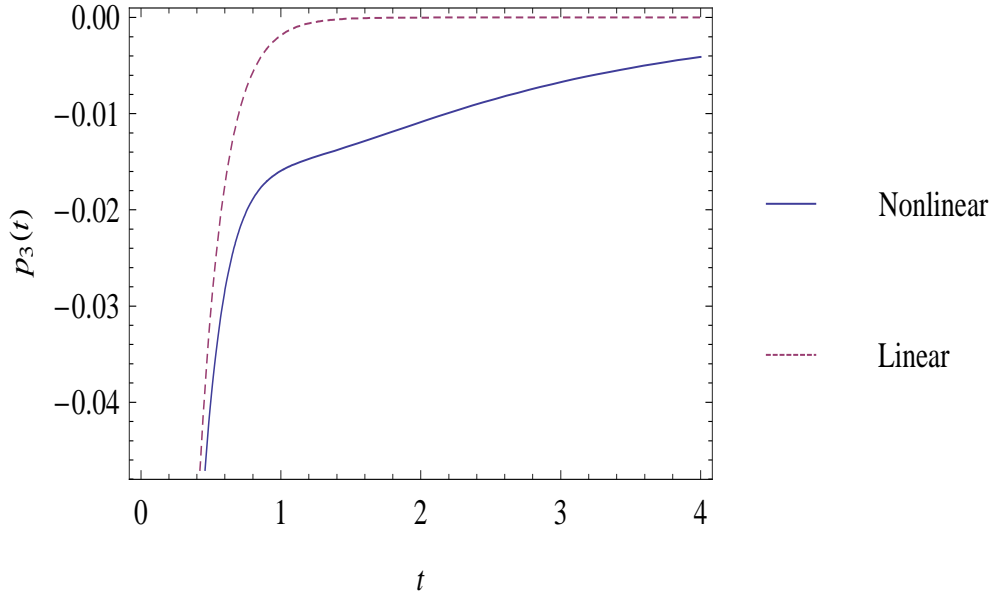


Figure 6.8. Variation of $p_3(t)$ coefficient in the linear and nonlinear simulations of Figure (6.2)

Though the previous two figures plot the net energy as a function of time, it might be helpful to plot individual energy of each mode and study the energy partitioning between them. This might provide some insight into the reasons for disagreement between linear and nonlinear results in some cases. Figures (6.3), (6.4) and (6.5) plot the variation of $p_1(t)$, $p_2(t)$ and $p_3(t)$ corresponding to the case of large difference between linear and nonlinear results. Similarly Figures (6.6), (6.7) and (6.8) plot the variation of $p_1(t)$, $p_2(t)$ and $p_3(t)$ corresponding to the case of small difference between linear and nonlinear results. Comparing these figures it can be seen that the differences are primarily due to $p_1(t)$ and $p_2(t)$ terms at later times.

6.4 Velocity Evolution With Time and Space

In this section we plot the spatial variation of the velocity (mean plus perturbation) in the physical domain at selected times. The parameters are taken to be $a = 0.2$, $\nu = 0.1$ and IC implemented were same as in Figure (6.1).

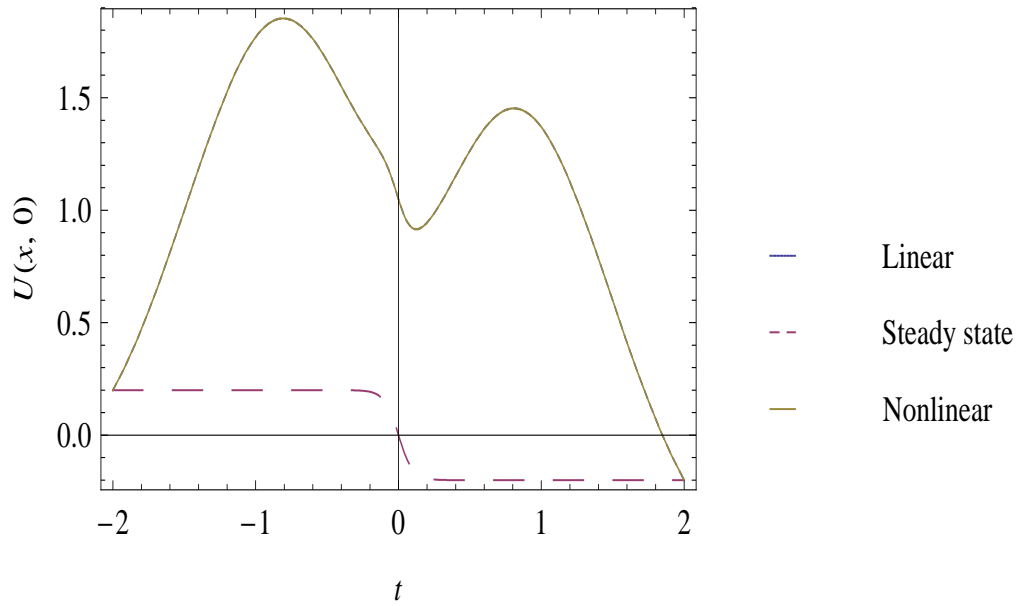


Figure 6.9. Plot showing the variation of velocity with respect to space for the linear and non-linear cases of Figure (6.1) at time $t=0$. The base flow is also plotted for reference in this and other figures next.

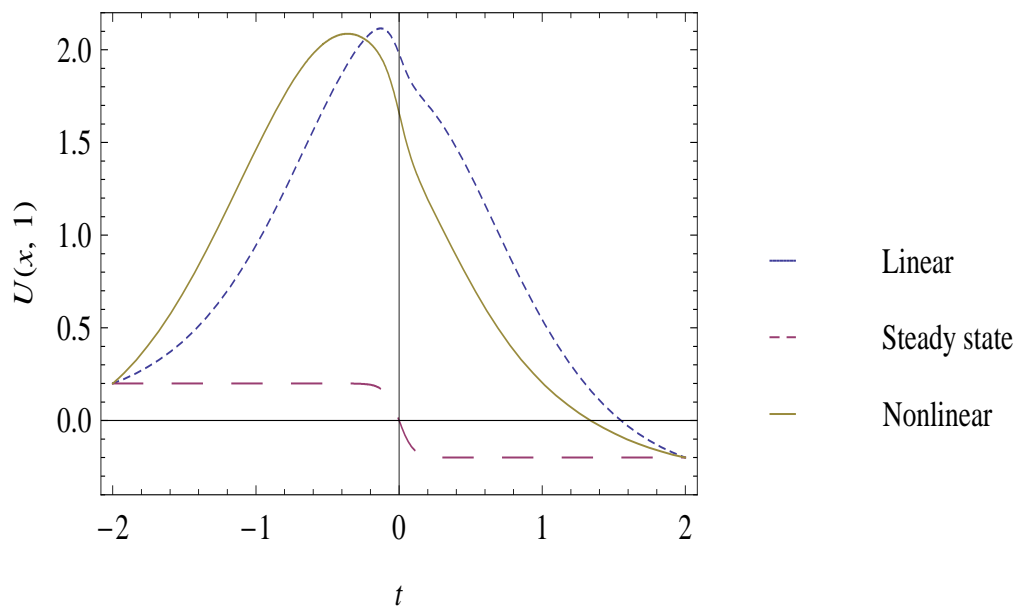


Figure 6.10. Plot showing the variation of velocity with respect to space for the linear and non-linear cases of Figure (6.1) at time $t=1$.

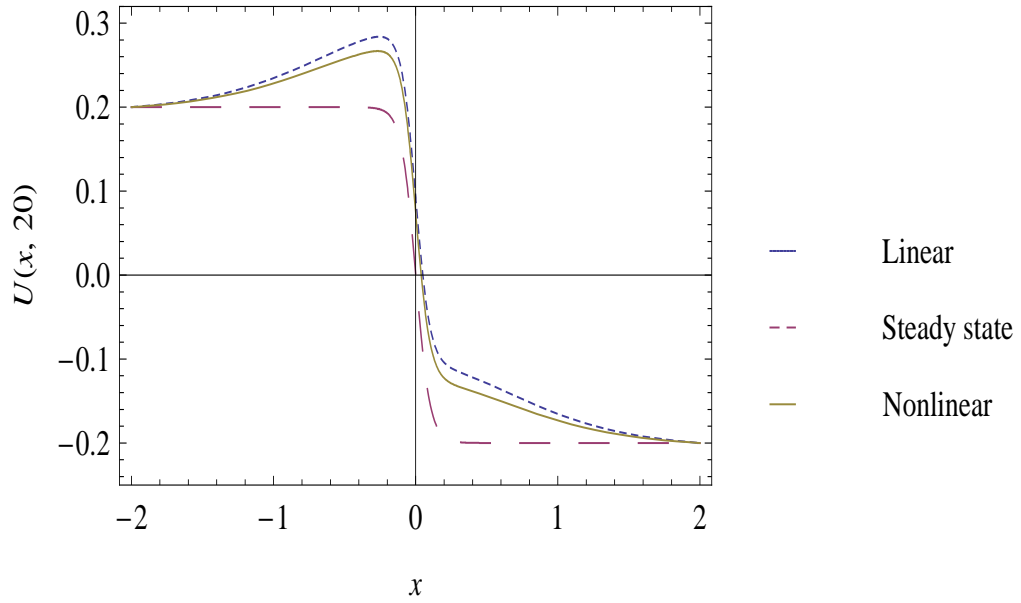


Figure 6.11. Plot showing the variation of velocity with respect to space for the linear and non-linear cases of Figure (6.1) at time $t=20$.

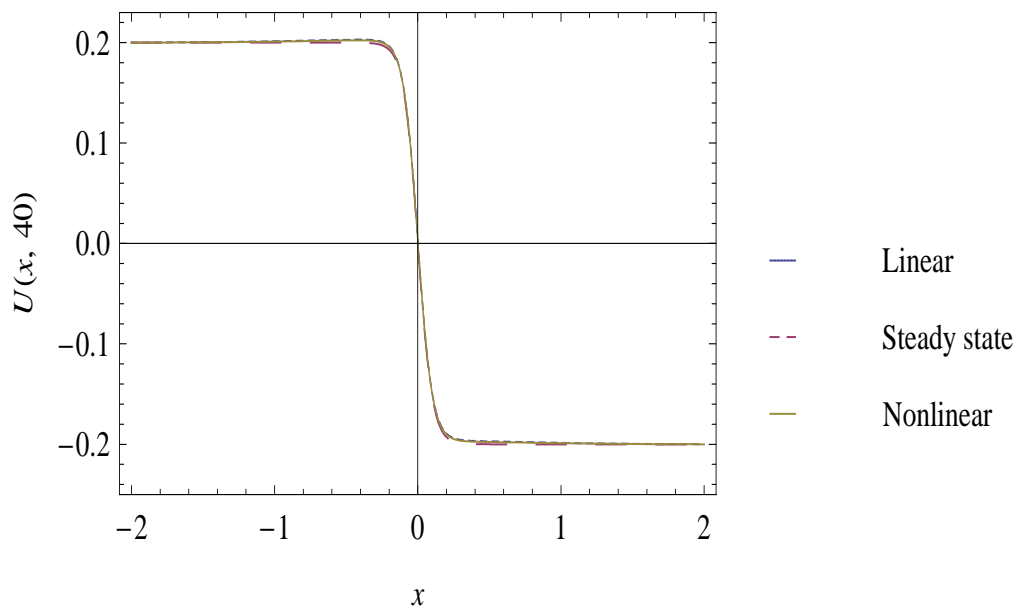


Figure 6.12. Plot showing the variation of velocity with respect to space for the linear and non-linear cases of Figure (6.1) at time $t=40$.

Figures (6.9), (6.10), (6.11) and (6.12) show the snapshots at $t = 0, 1, 20$ and 40. Note that as time passes by all perturbations decay in both linear and nonlinear simulations and hence indicating that the system might be globally nonlinearly stable.

CHAPTER 7

CONCLUSION AND SUMMARY OF MAIN RESULTS

In this thesis we studied the effect of spatial domain size, number of modes, non-hermitianness and non-normality on the stability and growth properties of a viscous, shock flow problem, as a prototypical example for the Navier-Stokes equations.

It has been shown that the above problems are not only non-normal but also non-hermitian, when the base flow has shear. The eigenvalue problems corresponding to infinite spatial domain, finite spatial domain, forward and L_2 adjoint problems are solved exactly by converting the linear partial differential equations into nonlinear Riccati equations. In the finite domain case, the full time dependent solutions are obtained analytically using the bi-orthogonal basis functions.

In the infinite spatial domain case, the point spectrum of the forward operator is shown to be unbounded and that of the adjoint operator to be empty. In the unbounded case, the spectrum fills the entire area on one side of a parabola in the complex plane and is connected. As the fluid viscosity decreases, the width of the parabola increases and in the limit of zero viscosity covers almost the entire left half plane. On the other hand, as the fluid viscosity increases, the width of the parabola decreases and in the limit of infinite viscosity becomes the negative real axis, which is the spectrum of the heat equation.

In the finite spatial domain case, the point spectrum lies in the open left half plane for all the Reynolds numbers and hence asymptotically stable. The results shown that perturbations grow substantially large for finite time before they decay at large times. It is also found that retaining right number of modes is crucial for

observing transient growth phenomena. Finally, the linear results are compared with the nonlinear finite amplitude simulation results.

Some of the questions that require further investigation are:

1. Is the shock flow problem globally nonlinearly stable as the numerics seem to indicate? Can this be proved analytically?
2. Calculating domain of attraction of the base state
3. Relevance of other stability notions
4. Studying periodic and unsteady base states stability of Burgers equation
5. Apply the above framework to instabilities and transition to turbulence problems of Navier-Stokes equations.
6. Use the above framework to design active feedback control laws for fluid flows.

BIBLIOGRAPHY

- [1] S. Chandrasekhar, *Hydrodynamic and Hydromagnetic Stability*, Dover Publications, New York (1981).
- [2] I. J. Wyganski, "On transition in a pipe," *Journal of Fluid Mechanics*, **59**, 281-335 (1973).
- [3] S. Davies, C. M. White, "An experimental study of flow of water in pipes of rectangular section," *Proc. Roy. Soc. London A*, **119**, 92-107 (1928).
- [4] N. Tillmark and P. H. Alfredsson, "Experiments on transition in plane couette flow," *Journal of Fluid Mechanics*, **235**, 89-102 (1992).
- [5] D. Meksyn and J. T. Stuart, "Stability of viscous motion between parallel planes for finite disturbances," *Proceedings at Royal Society of London A*, **208**, 517-526 (1951).
- [6] J. Watson, "On the nonlinear mechanics of wave disturbances in stable and unstable parallel flows part2," *Journal of Fluid Mechanics*, **9**, 371-389 (1961).
- [7] L. D. Landau, "On the problem of turbulence," *Dokl. Akad. Nauk SSSR* 44:311-314 (1944).
- [8] W. C. Reynolds and M. C. Potter, "Finite amplitude instability of parallel shear flows," *Journal of Fluid Mechanics*, **27**, 465-492 (1967).
- [9] C. L. Pekris and B. Scholler, "Stability of plane Poiseuille flow to periodic disturbances of finite amplitude," *Proceedings at National Academy of Sciences, USA*, **68**, 197-199, 1464-1435 (1971).

- [10] D. D. Joseph and S. Carmi, “Stability of poiseuille flow in pipes, annuli and channels,” *Quart. Appl. Math.*, **26**, 575-599 (1969).
- [11] K. Bobba, B. Bamieh and J. C. Doyle, Global stability and transient growth of stream-wise constant perturbations in plane Couette flow, *Phys. Fluids*, submitted
- [12] B. F. Farrell, “Optimal excitation of perturbations in viscous shear flow,” *Physics of Fluids*, **31**(8), 2093-2102 (1988).
- [13] M. T. Landahl, “Wave breakdown and turbulence,” *J. Appl. Math.*, **28**, 735-756 (1975).
- [14] T. Ellingsen and E. Palm, “Stability of linear flow,” *Physics of Fluids*, **18**(4), 487-488, (1975).
- [15] L. S. Hultgren and L. H. Gustavsson, “Algebraic growth of disturbances in a laminar boundary layer,” *Physics of Fluids*, **24**(6), 1000-1004 (1981).
- [16] L. H. Gustavsson, “Energy growth of three dimensional disturbances in plane poiseuille flow,” *Journal of Fluid Mechanics*, **224**, 241-260 (1991).
- [17] K. M. Butler and B. F. Farrell, “Three dimensional optimal perturbations in viscous shear flow,” *Physics of Fluids A*, **4**(8), 1637-1650 (1992).
- [18] S. C. Reddy, P. J. Schmid and D. S. Henningson, “Pseudospectra of Orr-Sommerfeld operator,” *SIAM Journal of Appl. Math.*, **53**, 15-47 (1993).
- [19] S. C. Reddy and D. S. Henningson, “Energy growth in viscous channel flows,” *Journal of Fluid Mechanics*, **252**, 209-238 (1993).
- [20] B. G. Klingmann, “On the transition due to three dimensional disturbances in plane poiseuille flow,” *Journal of Fluid Mechanics*, **240**, 167-195 (1992).

- [21] D. S. Henningson, A. Lundbladh and A. V. Johansson, “A mechanism for bypass transition from localized disturbances in wall bounded shear flows,” *Journal of Fluid Mechanics*, **250**, 169-207 (1993).
- [22] K. M. Bobba, “Lebesgue measures for transient response of the Navier-Stokes equations,” AIAA Paper No 2005-5061, 1-8, (2005).
- [23] K. M. Bobba, J. C. Doyle and M. Gharib, “Stochastic Input-Output Measures for Transition to Turbulence”, AIAA Paper No 2003-0786, 1-8 (2003).
- [24] K. Bobba, Robust Flow Stability: Theory, Computations and Experiments in Near Wall Turbulence, PhD Thesis, Caltech, Pasadena (2004).
- [25] J. M. Burgers, “A mathematical model illustrating the theory of turbulence,” *Advances in Applied Mechanics*, edited by R. Von Mises and Th. Von Karman, Vol 1, Academic Press, New York (1948).
- [26] E. Hopf, “The partial differential equation $u_t + uu_x = \mu u_{xx}$,” *Commun. Pure Appl. Math.*, **3**, 201 (1950).
- [27] J. D. Cole, “On a quasi-linear parabolic equation occurring in aerodynamics,” *Quart. Appl. Math.*, **9**, 225 (1951).
- [28] G. B. Witham, *Linear and Non-linear Waves*, Wiley and Sons (1974).
- [29] C. A. J. Fletcher, “Burgers equation: A model for all reasons, in Numerical Solutions of Partial Differential Equations”, page 139-225, J. Noyle, ed., North-Holland, Amsterdam-New York (1982).
- [30] R. H. Risch, “The problem of integration in finite terms,” *Transactions of the American Mathematical Society* **139**, 167 (1969).
- [31] G. K. Batchelor, *An Introduction to Fluid Dynamics*, Cambridge University Press, Cambridge (1967).

- [32] Q. Quarteroni, R. Sacco and F. Saleri, *Numerical Mathematics*, Springer-Verlag, New York (2000).
- [33] L. A. Segel, *Nonlinear Hydrodynamic Stability Theory*, University of Chicago Press (1966).
- [34] Reynolds, “On the dynamical theory of incompressible viscous fluids and the determination criterion,” *Phil. Trans. Roy. Soc. London(A)*, **186**, 123-164 (1895).
- [35] W. M. Orr, “The Stability or Instability of Unsteady motions of a liquid PART II: A viscous liquid,” *Proc. Roy. Irish Acad.(A)*, **27**, 69-138 (1907).
- [36] P. G. Drazin and W. H. Reid, “Hydrodynamic Stability,” *Cambridge University press* (1981).
- [37] Daniel D. Joseph, *Stability of Fluid motions I*, Springer Verlag, Berlin-Hiedelberg-Newyork (1976).
- [38] H. Bateman, H. Dryden, F. D. Murnaghan, *Hydrodynamics*, Dover Publications, NewYork (1936).
- [39] J. M. Burgers, *Advances in Applied Mechanics*, Academic Press, New York, Vol I (1948).
- [40] Wolfram Research, Inc., “Mathematica V 6.0,” *Wolfram Research* (2007).
- [41] J. S. Baggett and L. N. Trefthen, “Low Dimensional models for subcritical transition to turbulence,” *Physics of Fluids*, **9**, 1043-1053 (1997).